Extension of a printed circuit board and sample holder for experiments in circuit quantum electrodynamics

Semester Thesis

handed in at May 20, 2012

Swiss Federal Institute of Technology Zurich
Quantum Device Lab

Author	Samuel Häusler
Supervisor	Prof. Dr. Andreas Wallraff
Advisor	Dr. Matthias Baur

Abstract

In circuit quantum electrodynamics a small chip is used to study the matter light inter-
action. To access the chip it is placed on a printed circuit board which wires the chip to
coaxial cables. Prof. Andreas Wallraff and his group want to extend the chip for more
complex experiments. Therefore the printed circuit board and the sample holder around
it has to be extended as well.

The signal from the coaxial cables is guided with conductor-backed coplanar wave-
guides on the printed circuit board. To avoid unwanted electromagnetic modes vias
connect the top ground plane with the bottom ground plane. There are vias along the
waveguides called contour vias and such inside the contours called area vias. This work
presents a method to position the area vias efficiently.

In order to characterize the microwave properties of the printed circuit board and the
sample holder further boards were designed. A printed circuit board where neighbouring
ports are connected allows to measure the crosstalk. This board was produced in two
versions to study the effect of the area vias. One of them only contains contour vias
and the other also area vias. Another type of printed circuit board is equiped with
several capacitively coupled transmission lines serving as resonators. The boards are
used to recognize the disturbing electromagnetic resonances in the free space between
the printed circuit board, the sample holder and on the printed circuit board itself.

This printed boards have been measured with a network analyzer at room temperature
and in liquid nitrogen. For the measurement the printed circuit boards were connected
with coaxial cables to the analyzer. The influence of those cables has to be de-embedded.
For this aim generally usable formulas are given. The measured data of the printed
circuit board with resonators shows different types of resonances. A model is presented
to identify them.

The analysis suggests that area vias do not effect the transmission and crosstalk proper-
ties of the waveguides significantly. The contour vias seem to be sufficient. The crosstalk
is attenuated by about $50\,\mathrm{dB}$.

Contents

1. Introduction

The fundamental interaction between matter and light can be studied in experiments in circuit quantum electrodynamics. The matter is implemented by a superconducting cooper pair box, acting as an artificial atom, located near a resonator. The resonator can trap microwave photons which interact with the cooper pair box. The cooper pair box and the resonator are placed on a *chip* with a size of about several millimeters. Since the chip is small a *printed circuit board* (PCB) is needed to connect the resonator and other features on the chip to coaxial cables. The chip has to be protected against interfering electromagnetic fields. Therefore the PCB and the chip are enclosed by a *sample holder* made of cooper. Figure 1.1 shows a schematic overview. Between the PCB and the sample holder is still free space, which allows unwanted electromagnetic modes to establish. These modes can be suppressed by filling the space with a piece of metal, called *cover*.

The goals of the work are the following.

1. So far Professor Wallraff and his group used a PCB and a sample holder designed for eight coaxial cables. To study more complex "matter" light interactions the PCB and the sample holder should be extended to sixteen cables.

2. On the PCB the microwaves are guided by waveguides. To suppress unwanted modes in the waveguides, so called via holes are placed on the PCB. Since they are expensive one is interested to know how to distribute them properly.

3. The new sample holder and the new PCB should be characterized. For this purpose the parasitic resonance frequencies should be measured when no cover suppresses them and the cross coupling between different waveguides on the PCB should be specified.
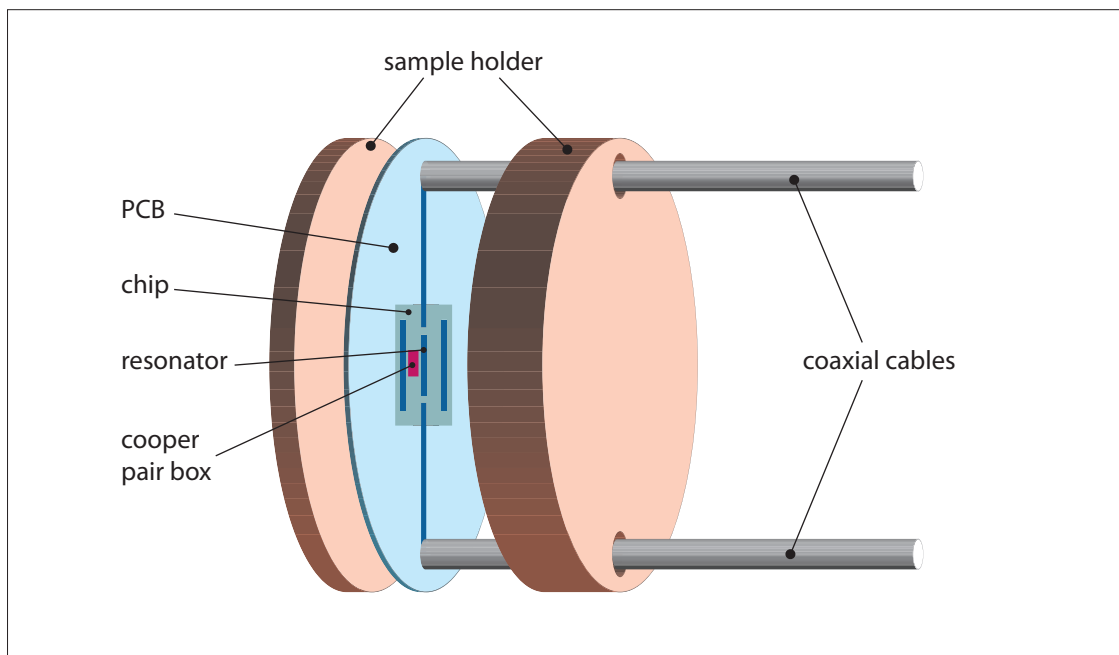
Figure 1.1.: A superconducting cooper pair box is located near a resonator. They are placed on a chip which is mounted on a PCB. The PCB connects the chip to coaxial cables. The PCB and the chip are enclosed by a sample holder.

2. Design of the PCB

Figure 2.1 shows the previous PCB design. The hole in the middle leaves room to hold the chip. From there eight waveguides drawn in black lines go outwards to the connectors. The red holes at the edge of the PCB are used to screw the PCB on the sample holder.

The aim is to extend the PCB from eight connectors to sixteen. To create space for the additional connectors the diameter of the PCB is increased. It has to fulfill the following requirements.

- The PCB leads the electromagnetic pulses from the coaxial cables to the chip and back. The microwave pulses have to be transmitted without interfering reflections. The different waveguides should crosstalk as little as possible.

- The chips vary in their size and the number and position of their pins. PCBs are required that support these different chips.

The next sections discuss the different parts on the PCB.

2.1. Waveguides

2.1.1. Different types

There are several types of waveguides. Two of them are the conventional coplanar waveguide and the conductor-backed coplanar waveguide. The conventional coplanar waveguide consists of a dielectric and a thin conducting film on the top (figure 2.2a). The conducting film is split into three parts. The outer parts are grounded and the signal voltage is applied to the center strip. The applied voltage causes an electromagnetic wave which propagates perpendicular to the image plane. The electric field lines are shown in figure 2.2c. The conductor-backed coplanar waveguide has an additional ground plane at the bottom of the dielectric (figure 2.2b). Figure 2.2d shows the electric field lines. [7, page 1, page 87]

The waveguides on the PCB are designed as conductor-backed coplanar waveguides. The width of the center strip s is chosen as $150\,\mu\text{m}$ and the distance between the center strip and the ground plane w is $90\,\mu\text{m}$. The dielectric material is AD1000 produced by Arlon-Microwave Materials. It has a relative dielectric constant ϵ_r of 10 ± 0.35 at $10\,\text{GHz}$ [1, page 3] and a thickness of $20\,\text{mils}$ ($\approx 0.5\,\text{mm}$).

2.1.2. Bends

The waveguides in the used PCB design are bent (figure 2.1). This type of bend is called swept bend. Bends present discontinuities for the propagating microwave signal and a
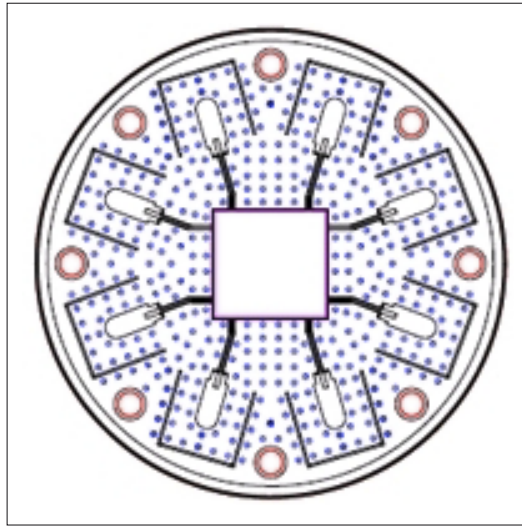
Figure 2.1.: Previous PCB design with a chip hole [6, page 14]
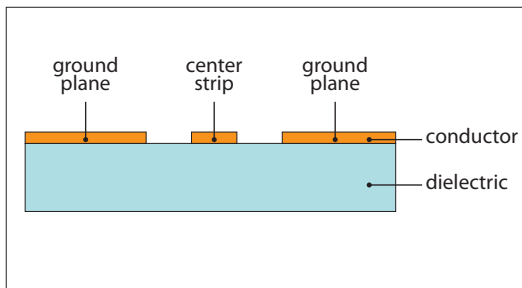
(a) Cross section through a conventional coplanar waveguide

(b) Cross section through a conductor-backed coplanar waveguide

(c) Electric field lines of a conventional coplanar waveguide. Drawn according [7, page 61]

(d) Electric field lines of a conductor-backed coplanar waveguide. Drawn according [7, page 95]

Figure 2.2.: Different types of waveguides

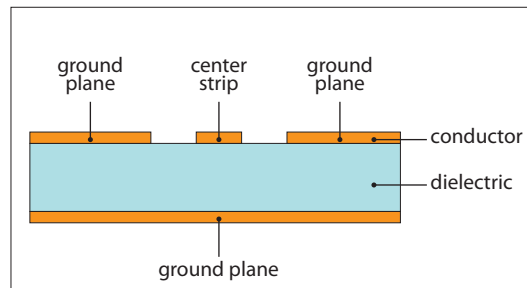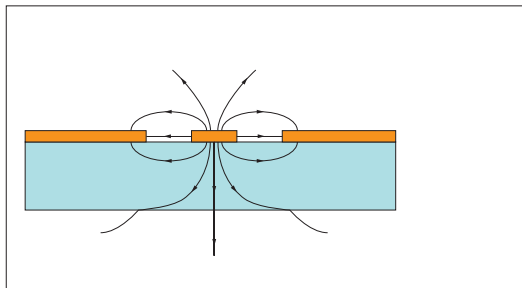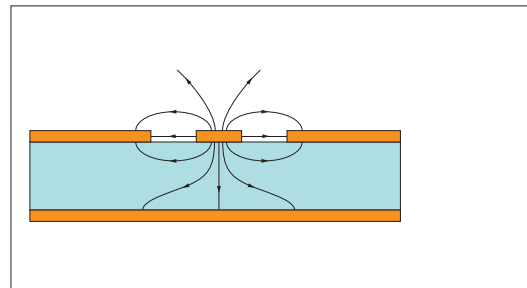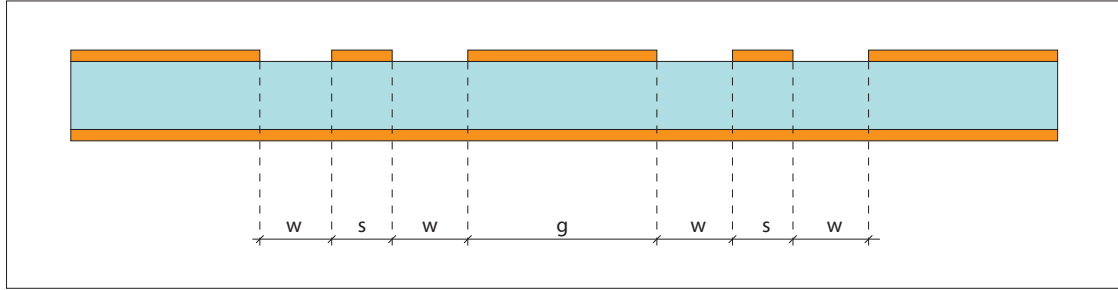Figure 2.3.: Cross section through adjacent conductor-backed coplanar waveguides

part of the signal is reflected. This lowers the transmission of the signal. The following design rule helps to minimize the reflections[1].

$$r \geq 10s \tag{2.1}$$

The minimal radius r is therefore 1.5 mm for the value s given in section 2.1.1.

2.1.3. Coupling between two waveguides

Figure 2.3 shows a cross section through two parallel conductor-backed coplanar waveguides. The coupling between them can be minimized by separate them as far as possible. The following design rule helps to choose the separation g [8, page 41].

$$g \geq 2w + s \tag{2.2}$$

This gives a minimal separation g of 330 µm for the values of s and w given in section 2.1.1. According to the reference the coupling is up to 40 GHz lower than -30 dB for even modes and lower than -20 dB for odd modes.

2.1.4. Connectors on the PCB

Figure 2.4 shows how the PCB is connected to a coaxial cable. The PCB connector is soldered on the PCB such that the pin of the connector touches the center strip of the waveguide but not the ground plane around the center strip. Otherwise the waveguide is shorted. The female-female bullet is mounted into the PCB connector. The coaxial cable is directly plugged into the bullet. The solder paste is SC170 of the company Solder Chemistry. The PCB connector 19S102-40ML5 and the female-female bullet are from Rosenberger.

2.2. Vias

The transmission characteristic of the conductor-backed coplanar waveguide can be improved by vias. Vias are plated through holes connecting the top ground plane with the

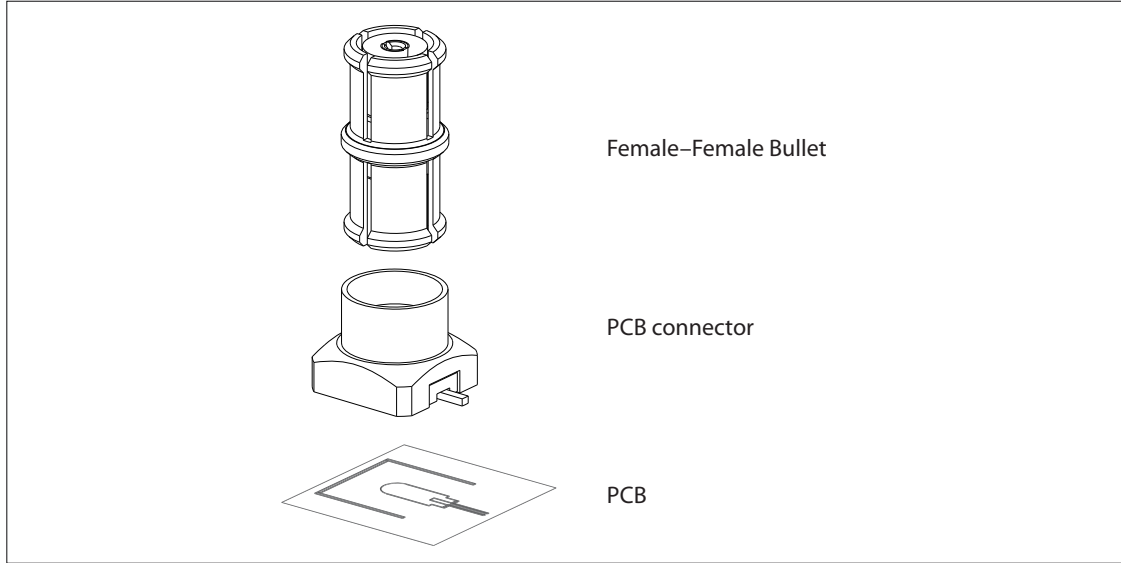---

[1]Recommendation of Lars Steffen

Figure 2.4.: Electrical connection from the PCB to a coaxial cable. The PCB connector is soldered onto the PCB, the outer contact to the PCB ground plane and the inner contact to a waveguide center strip. The female-female bullet is required because the coaxial cables are fitted with male connectors.

bottom ground plane. In this work vias along the contour of the waveguides are called *contour vias* and vias between the waveguides are called *area vias* (figure 2.5). Vias can improve the following points.

- The top ground plane and the bottom ground plane have to have the same potential. This can be achieved with vias. Otherwise there can occur interfering modes between the ground planes called parallel plate line modes. [9]

- Contour vias restrict the modes sidewards. If the distance L is small enough the waveguide can be modeled as a rectangular waveguide with two slots in the top wall (figure 2.5 and [9]). This decreases the crosstalk between neighbouring waveguides.

The contour vias should be placed as close to the center pin as possible [9]. It is unclear if the area vias are necessary. One aim of this work is to clarify their impact on the microwave properties. To this end a PCB only with contour vias was produced and another with additional area vias. In order to design a PCB with area vias we have to think about how to place them efficiently.

2.2.1. Positioning of area vias

Consider the following situation. The contour vias are already placed and the area vias should be added within a certain region. The positioning should respect the following conditions.
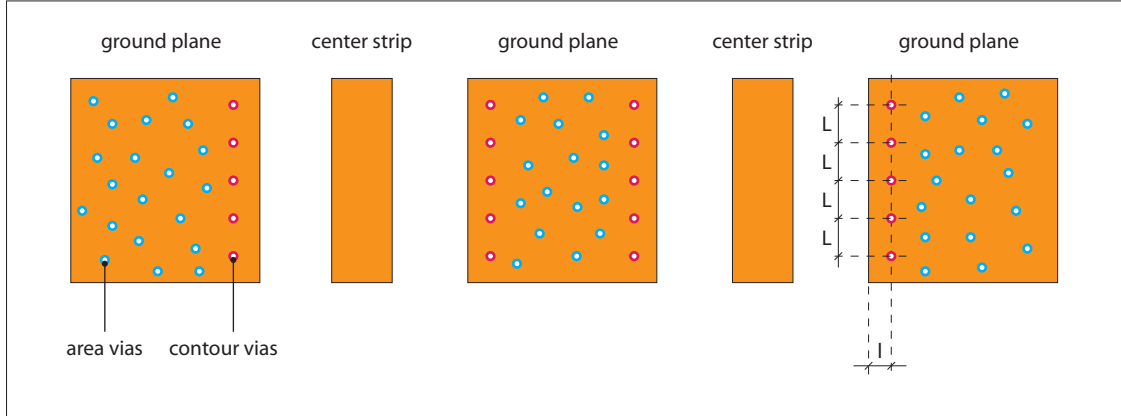
Figure 2.5.: Top view on two conductor-backed coplanar waveguides

- The area vias should be distributed homogeneously and dense. This is a promising way to suppress the parallel plate line modes.

- Adjacent vias should be enough separated because it is technically impossible to place them arbitrarily close together.

- Vias are expensive. Thus they should be placed economically.

A practical way to position them is inspired by the plant impatiens noli-tangere. Impatiens noli-tangere contains their seed in a capsule and they are spread explosively around the plant (figure 2.6). New plants grow and distribute their seeds in the same manner. This translates to the algorithm 1. The polygon P defines the region where the area vias should be spread. The set V contains the positions of the contour vias. This gives the starting situation sketched in figure 2.7a. Pick a via from the set V and generate randomly n positions around this via. The distance from the originating via should be greater than minDist and smaller than maxDist (figure 2.7b). Proposed positions which are too close to another via are discarded. The remaining positions are added to the set V. Now take the next via and repeat the procedure until all vias have spread their "seeds". At the end the set V contains the positions of the new area vias. Figure 2.7c shows a possible distribution.

The PCBs are designed with AutoCAD 2011. It is therefore handy to export the polygon P and the positions of the contour vias V with AutoCAD into text files. The text files are processed with Octave functions which place the area vias with the impatiens algorithm. The output is written into a text file. AutoLISP routines read it and draw the vias directly in AutoCAD. The positions of the area vias can then be adapted if needed. Figure 2.8 shows the data flow. A user manual can be found in appendix A.

The new PCBs are bigger than the previous ones and therefore more area vias are required. The program speeds up their placement.

In the new designs the distance l is 310 μm and L is about 1.0 mm (figure 2.5). The parameters minDist and maxDist are chosen as 0.8 mm respectively 1.2 mm. The number n

(a) flower   (b) closed capsule   (c) opened capsule

Figure 2.6.: Impatiens noli-tangere. With kind permission of Prof. Paul Busselen from the Catholic University in Leuven.
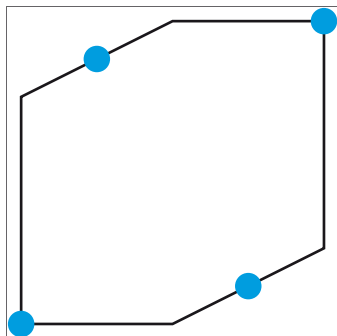
(a) At start a polygon defines the region where area vias shall be placed. The contour vias are preset (blue dots).
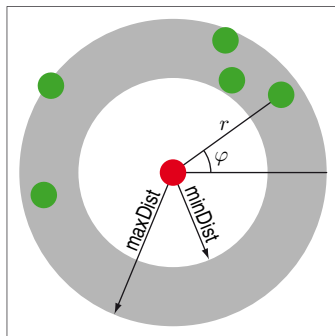
(b) Around a placed via (red dot) new area via positions (green dots) are randomly proposed within the gray shaded ring.
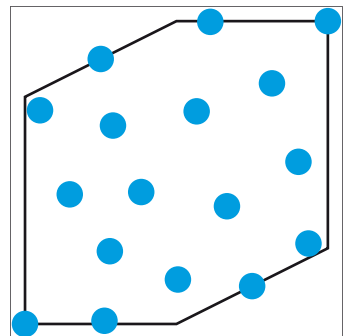
(c) At the end the polygon is filled with area vias.

Figure 2.7.: Impatiens algorithm

Algorithm 1 Impatiens Algorithm

1: **function** ADDVIAS(polygon P, contour vias V, integer n, real: minDist, maxDist)
2:      $i \leftarrow 1$
3:      **while** $i \leq |V|$ **do**
4:          $C \leftarrow n$ randomly chosen positions c with minDist $\leq \|V(i) - c\| \leq$ maxDist
5:          **for all** $c \in C$ **do**
6:              **if** $c \in P \wedge \min\{\|c - v\| : v \in V\} \geq$ minDist **then**
7:                  append c to V
8:              **end if**
9:          **end for**
10:         $i \leftarrow i + 1$
11:      **end while**
12:      **return** V
13: **end function**
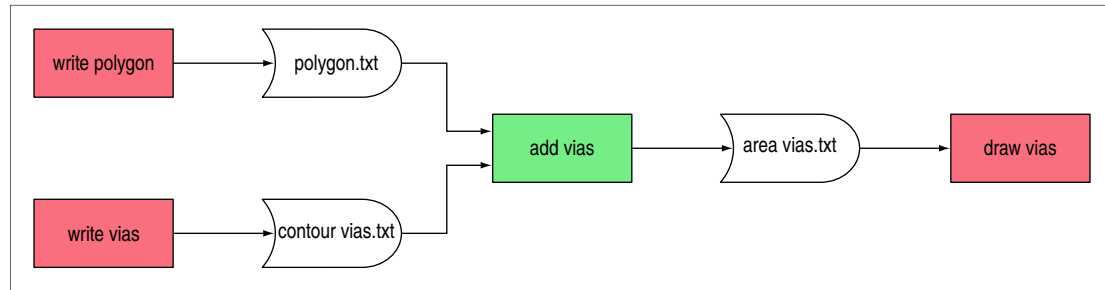
Figure 2.8.: The polygon and the contour via positions are exported from AutoCAD 2011 into text files. The text files are processed by Octave functions which place and outputs the new area vias. The output file is read by AutoCAD to draw the new vias.

is around 40. The total number of via holes can be adjusted by varying n.

2.3. New PCB designs

The new PCBs have sixteen connectors and a diameter of 49.8 mm. They are produced by Hughes Circuits, Inc.

There are three different types of PCB designs.

1. PCBs for experiments in circuit quantum electrodynamics hold a chip in the *chip hole* in the middle of the PCB.

2. PCBs with *resonators* allows to characterize parasitic modes.

3. PCBs with neighbouring ports connected with a *through* are used to measure the crosstalk and the influence of the area vias.

2.3.1. PCB with chip holes

Figure 2.9 shows the designed PCBs with chip holes. Vias are represented by blue circles, the waveguides and the space for connectors with black lines. The red circles at the edge are holes to screw the PCB on the sample holder.

2.3.2. PCB with resonators

Figure 2.10 shows the PCB with resonators. Each resonator has a length l of 12.5 mm. The lowest resonance frequency $\nu_{\min}$ is given by the dispersion relation with a wavelength of $2l$.

$$2l\nu_{\min} = v_{\text{ph}} \tag{2.3}$$

The phase velocity v_{ph} is given with the vacuum light speed c and the effective dielectric constant ϵ_{eff} as

$$v_{\text{ph}} = \frac{c}{\sqrt{\epsilon_{\text{eff}}}}. \tag{2.4}$$

The effective dielectric constant can be calculated with

$$\epsilon_{\text{eff}} \approx \frac{1 + \epsilon_{\text{r}}}{2} \tag{2.5}$$

in case that the dielectric is much thicker than $w + {}^s\!/_2$ [6, page 5]. This is fulfilled since the dielectric is about 0.5 mm thick, the center strip has a width s of 150 µm and w is 90 µm (see section 2.1.1). The relative dielectric constant ϵ_{r} is 10 and therefore the effective dielectric constant ϵ_{eff} approximately 5.5.

Together with formula (2.3) this gives a lowest resonance frequency $\nu_{\min}$ of 5.1 GHz. Further resonator resonances are expected at multiples of $\nu_{\min}$ (10.2 GHz, 15.3 GHz, . . .).

2.3.3. PCB with throughs

Figure 2.11 shows the two PCB designs with throughs. One version only contains contour vias and the other one has additional area vias.
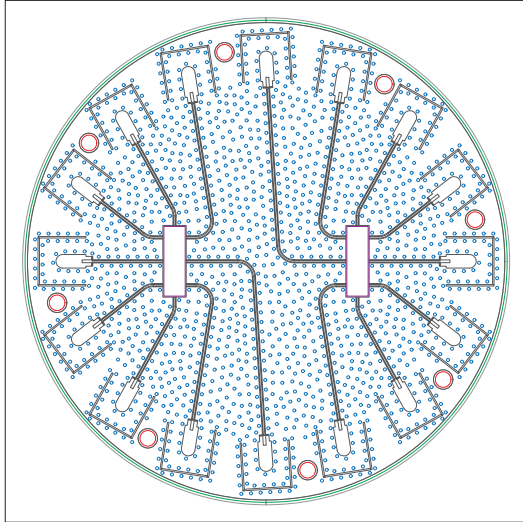
(a) PCB for two chips of size $2.0\,\text{mm} \times 7.0\,\text{mm}$
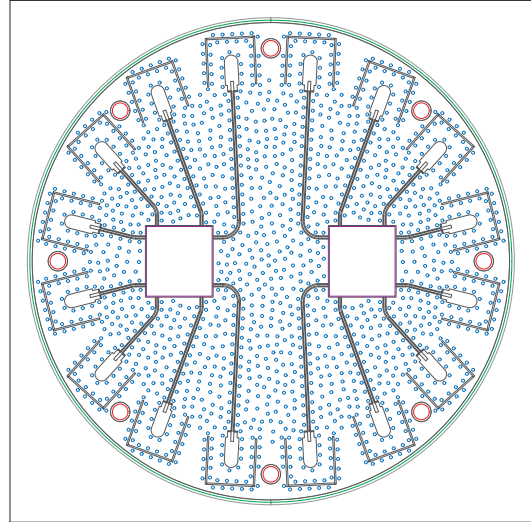
(b) PCB for two chips of size $6.6\,\text{mm} \times 7.0\,\text{mm}$
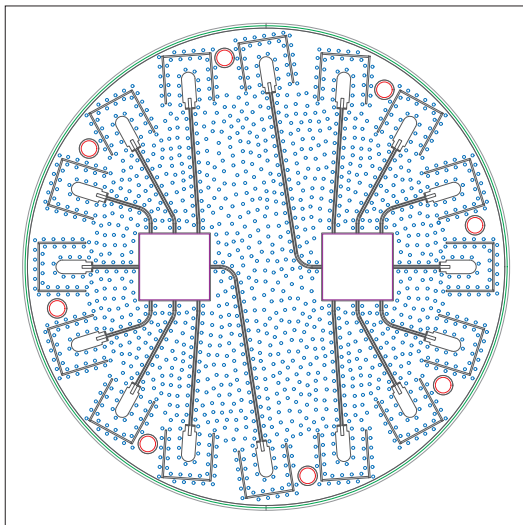
(c) PCB for two chips of size $6.6\,\text{mm} \times 7.0\,\text{mm}$
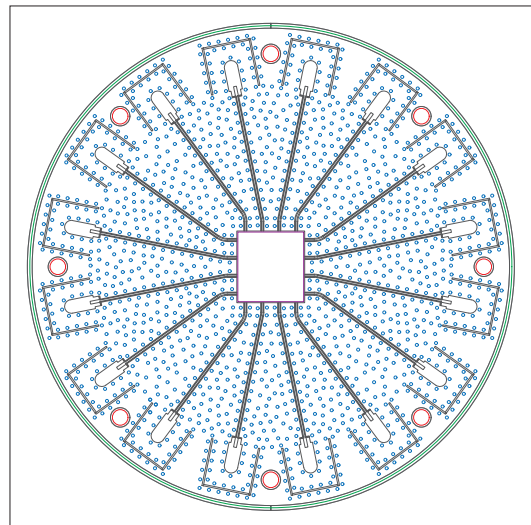
(d) PCB for one chip of size $6.6\,\text{mm} \times 7.0\,\text{mm}$

Figure 2.9.: New PCB designs with chip holes

Figure 2.10.: New PCB design with resonators
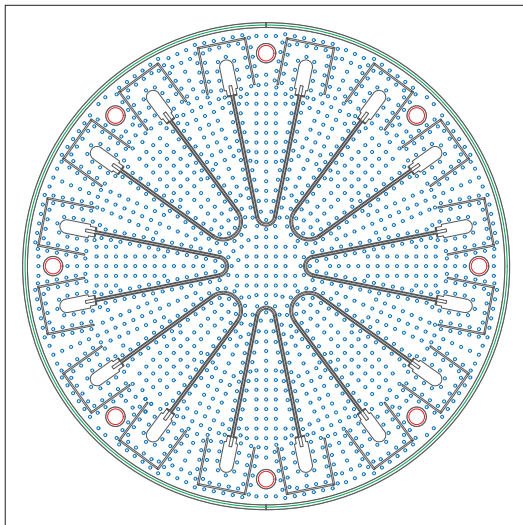
(a) PCB with throughs, contour and area vias
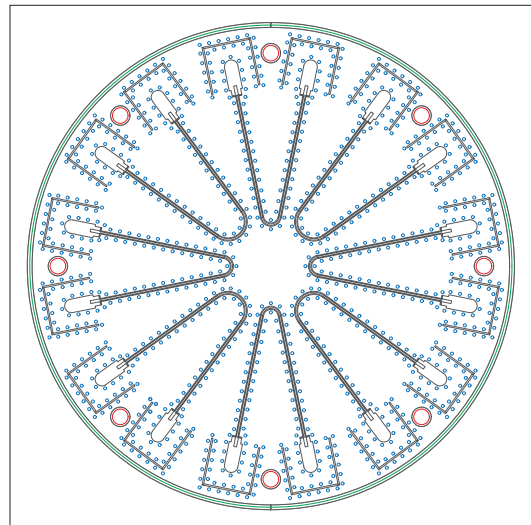
(b) PCB with throughs and contour vias

Figure 2.11.: New PCB designs with throughs. The waveguides are designed as shown in 2.9d except for the bends in the center.

3. Sample holder

The sample holder encloses the PCB to suppress interfering electromagnetic fields from the environment. Since the new PCB is extended from eight to sixteen connectors the sample holder has to be extended as well. Martin Goeppel designed the sample holder for eight connectors with AutoCAD Inventor. Figure 3.1 shows an exploded drawing of the extended sample holder consisting of the lid and the mount, the PCB and the coils.

These parts are assembled as follows. First the PCB with the connectors and the bullets is screwed onto the mount. Then the coaxial cables are connected through the holes in the lid and mechanically fixed. Now the mount is pushed into the lid and they are screwed together. Two small coils or one big coil can be screwed onto the mount. The coils are used to tune the transition frequency of the superconducting cooper pair box. In this work the coils are not used since only the sample holder and the PCBs are characterized.

The sample holder was produced by the ETH internal apprenticeship workshop according to the plan in appendix B.
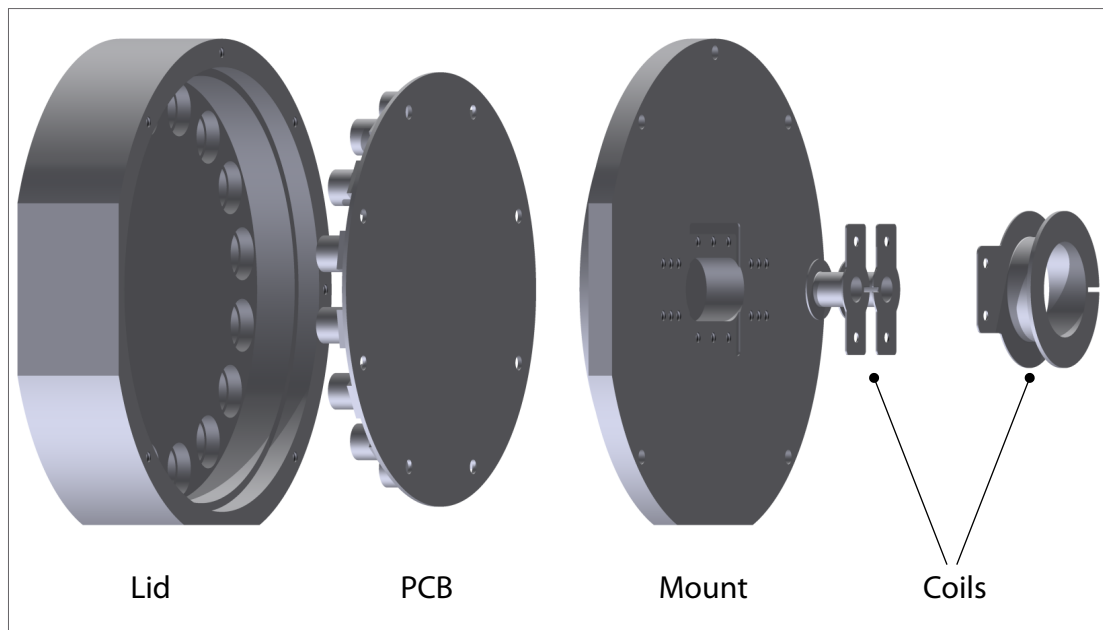
Figure 3.1.: Exploded drawing of the sample holder, the PCB and the coils

4. Measurement

The electrical properties of a PCB enclosed by the sample holder can be characterized by S-parameters. The following chapter describes how they can be measured with a network analyzer. For the measurement a microwave network analyzer N5230C PNA-L from Agilent Technology was used.

4.1. Setup

The device under test consists of the coaxial cables and the PCB enclosed by the sample holder. The coaxial cables run through a metallic tube called dipstick. The dipstick allows to cool the sample holder in liquid nitrogen or in a cryostat. The network analyzer ports are connected to the coaxial cables by measurement cables (see figure 4.1).

The network analyzer measures now the network with the four ports A, B, C and D. Since we are interested in the network with the ports 1, 2, 3 and 4 the effects of the measurement cables and the coaxial cables have to be de-embedded.

4.2. Calibration

The measurement cables can be de-embedded by calibrating the network analyzer. For this purpose the measurement cables are attached to the network analyzer and on the other side to the four port electronic calibration module N4433A from Agilent Technology. The calibration is done automatically.

The coaxial cables can not be calibrated with the electronic calibration module since the connectors do not fit. Therefore the S-parameters of each coaxial cable is measured separately in a two port measurement. The effect of the coaxial cables can be de-embedded numerically (see section 5.1). This calibration scheme presumes that the crosstalk between the coaxial cables is negligible.

The S-parameters of the coaxial cables differ generally. Therefore it is important to always plug the same coaxial cable into the same port of the PCB.

4.3. Measurement

The PCBs shown in figure 4.2 are examined from $300\,\mathrm{kHz}$ up to $20\,\mathrm{GHz}$. Each PCB is measured at room temperature of about $300\,\mathrm{K}$ and in liquid nitrogen at $77\,\mathrm{K}$.
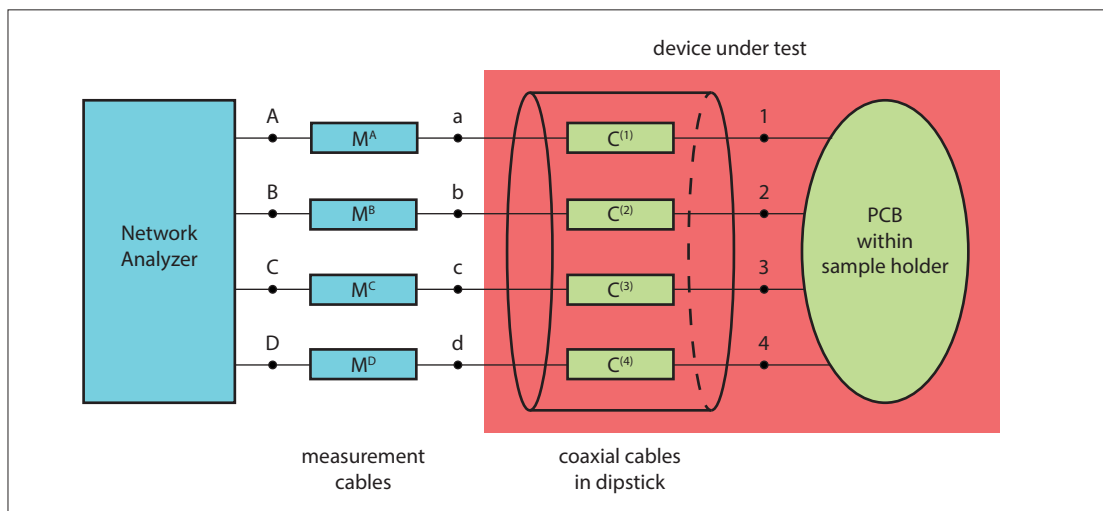
Figure 4.1.: The device under test consists of coaxial cables in the dipstick and the PCB enclosed by the sample holder. It is connected with measurement cables to the network analyzer.
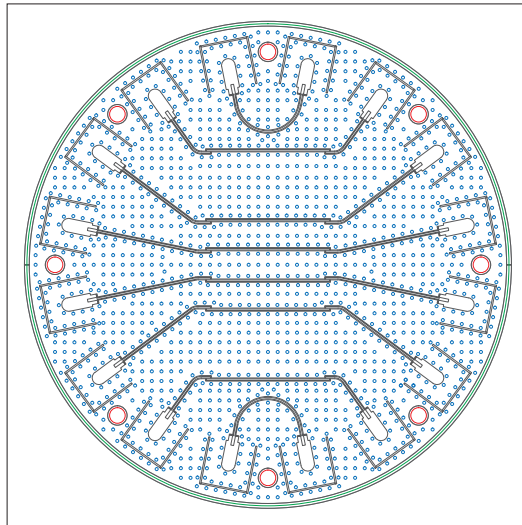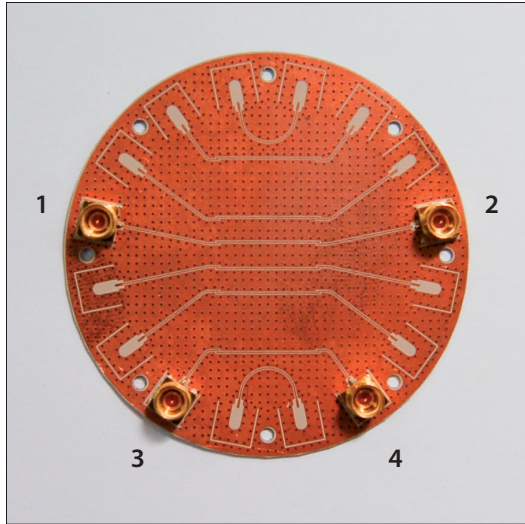
(a) PCB with resonators
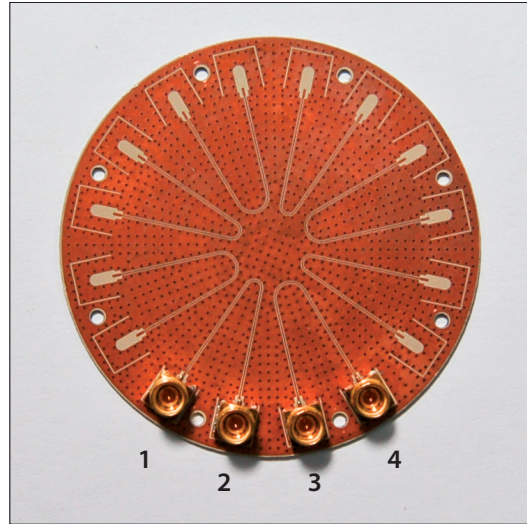
(b) PCB with throughs, contour and area vias
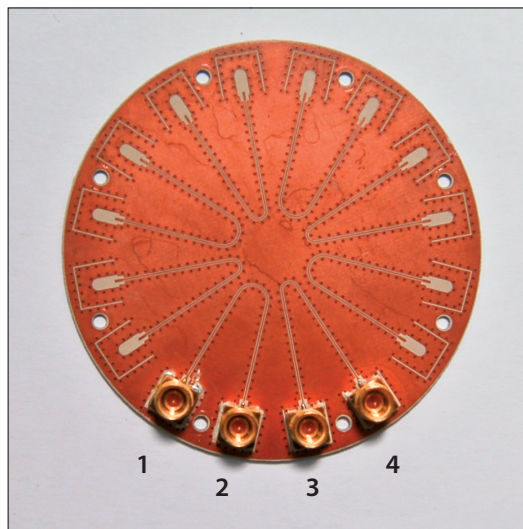
(c) PCB with throughs and contour vias

Figure 4.2.: Measured PCBs with connectors

5. Analysis and Discussion

5.1. De-embedding the coaxial cables

The network analyzer measures the following S-matrices.

- The four port a, b, c and d (see figure 4.1) is described by the four by four matrix $\mathbf{S}^{\mathrm{m}}$.

- The coaxial cables are described by the two by two matrices $\mathbf{C}^{(1)}$, $\mathbf{C}^{(2)}$, $\mathbf{C}^{(3)}$ and $\mathbf{C}^{(4)}$.

With the measured S-parameters the four by four S-matrix $\mathbf{S}^{\mathrm{d}}$ of the PCB within the sample holder is given by the linear equation

$$\mathbf{M}(\mathbf{S}^{\mathrm{d}})^{\mathrm{T}} = \mathbf{B}, \tag{5.1}$$

with the matrices

$$\mathbf{M}_{ij} = \frac{\mathbf{C}_{22}^{(j)}\mathbf{S}_{ji}^{\mathrm{m}} - \delta_{ij}\det(\mathbf{C}^{(i)})}{\mathbf{C}_{12}^{(j)}}, \tag{5.2}$$

$$\mathbf{B}_{ij} = \frac{\mathbf{S}_{ji}^{\mathrm{m}} - \delta_{ij}\mathbf{C}_{11}^{(i)}}{\mathbf{C}_{12}^{(j)}} \quad \text{and} \tag{5.3}$$

$$\delta_{ij} = \begin{cases} 1, & \text{for } i = j \\ 0, & \text{for } i \neq j \end{cases}. \tag{5.4}$$

The derivation of the equations can be found in appendix C. They are not only valid for four by four S-matrices but also for n by n matrices. The coaxial cables were de-embedded from the measured S-parameters with Mathematica.

5.2. Analysis of the PCB with resonators

The magnitude $\mathbf{S}_{12}$ of a resonator looks typically as shown in figure 5.1. The peaks and dips come from resonances in the sample holder and from the resonator on the PCB. They can be identified with the following simple model.
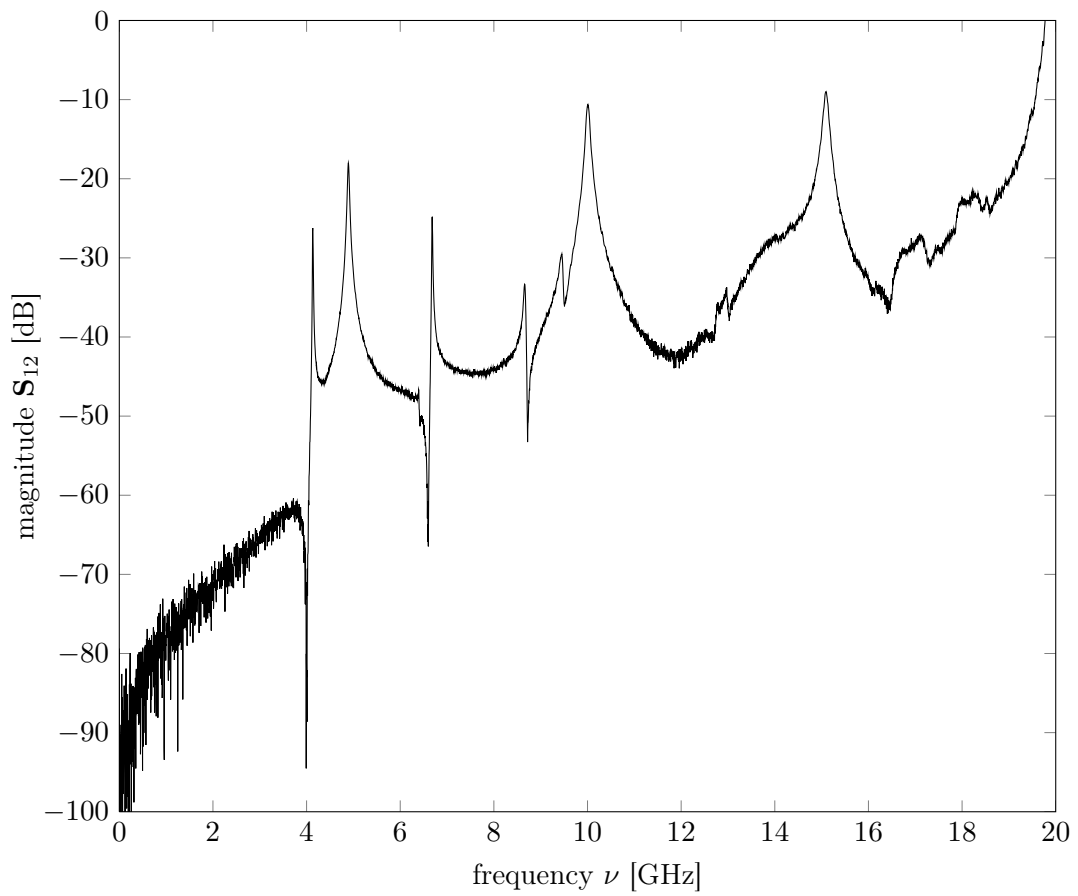
Figure 5.1.: Magnitude $\mathbf{S}_{12}$ of PCB shown in figure 4.2a at 77 K
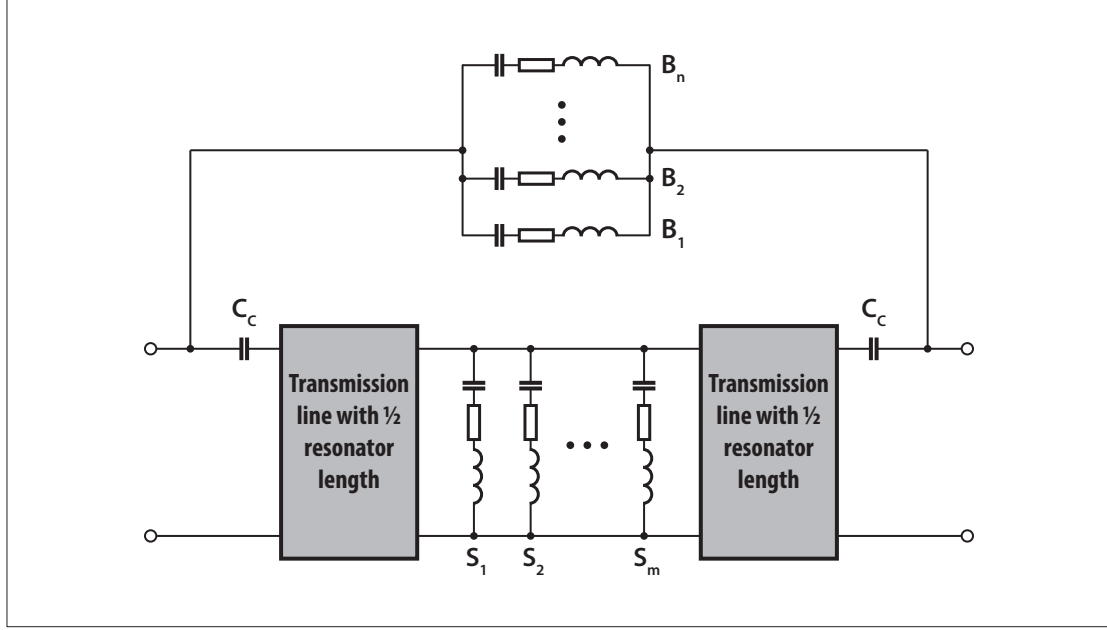
Figure 5.2.: Simple model of a PCB resonator in a sample holder

5.2.1. Resonance model

The PCB with resonators within the sample holder can be modeled with the circuit shown in figure 5.2. The coupling capacitances C_c and the transmission lines simulate the resonator on the PCB [2, page 10 et seq.]. The sample holder resonances can be modeled with series resonant circuits. The series resonant circuits B_i bridges the transmission line at resonance, therefore they are called *bridging series resonant circuits*. They are motivated by electromagnetic modes which bypass the resonator. The series resonant circuits S_i shunt the transmission line at resonance, so they are called *shunting series resonant circuits*. They model modes which load the resonator and reduce its energy. This shunts could be located anywhere along the resonator. To simplify the model we assume that they are located in the middle.

S-parameters of the model circuit

The S-matrix of the equivalent circuit can be calculated with the four-port network analysis. Each series resonant circuit is described by the capacitance C, the resistance R and the inductance L. The resonance frequency ν_s is the frequency where the impedance of the circuit becomes minimal. It is given by

$$\nu_s = \frac{1}{2\pi\sqrt{LC}}. \tag{5.5}$$

The quality factor Q of the series resonant circuit is

$$Q = 2\pi\nu_s \frac{L}{R}. \tag{5.6}$$

The admittance Y of the series resonant circuit can be written as

$$Y = \mathrm{i}2\pi\nu C \frac{(\nu_\mathrm{s}^2 - \nu^2)Q - \mathrm{i}\nu_\mathrm{s}\nu}{[(\nu_\mathrm{s}^2 - \nu^2)Q]^2 + \nu_\mathrm{s}^2\nu^2}\nu_\mathrm{s}^2 Q. \tag{5.7}$$

The formulas (5.5), (5.6) and (5.7) are derived in the appendix D.

With this the ABCD-matrix of the transmission line and the shunting series resonant circuits is given by

$$\mathbf{A} = \mathbf{A}_c \cdot \mathbf{A}_\mathrm{TL} \cdot \begin{pmatrix} 1 & 0 \\ \sum_{i=1}^{m} Y(S_i) & 1 \end{pmatrix} \cdot \mathbf{A}_\mathrm{TL} \cdot \mathbf{A}_c, \tag{5.8}$$

with the matrices

$$\mathbf{A}_c = \begin{pmatrix} 1 & (\mathrm{i}2\pi\nu C_c)^{-1} \\ 0 & 1 \end{pmatrix} \quad \text{and} \tag{5.9}$$

$$\mathbf{A}_\mathrm{TL} = \begin{pmatrix} \cosh(\gamma l/2) & Z_0\sinh(\gamma l/2) \\ \sinh(\gamma l/2)/Z_0 & \cosh(\gamma l/2) \end{pmatrix}. \tag{5.10}$$

The quantity Z_0 denotes the characteristic impedance of the transmission line. It is usually $50\,\Omega$. The transmission line on the PCB between the gaps has a length l and a propagation constant γ given by

$$\gamma = \alpha + \mathrm{i}\frac{2\pi\nu}{v_\mathrm{ph}}, \tag{5.11}$$

with the attenuation constant α and the phase velocity v_ph. The ABCD-matrix $\mathbf{A}_\mathrm{TL}$ is derived in the appendix E. The ABCD-matrix $\mathbf{A}$ can be converted into the admittance matrix. This admittance matrix can simply be added with the admittance matrix of the bridging branch to obtain the admittance matrix of the total circuit.

$$\mathbf{Y} = \frac{1}{\mathbf{A}_{12}}\begin{pmatrix} \mathbf{A}_{22} & -\det(\mathbf{A}) \\ -1 & \mathbf{A}_{11} \end{pmatrix} + \sum_{i=1}^{n} Y(B_i)\begin{pmatrix} 1 & -1 \\ -1 & 1 \end{pmatrix}. \tag{5.12}$$

The admittance matrix $\mathbf{Y}$ of the circuit can be converted into the S-matrix $\mathbf{S}$ with the following formula

$$\mathbf{S}_{11} = \frac{\mathbf{A}_{11} + \mathbf{A}_{12}/Z_0 - \mathbf{A}_{21}Z_0 - \mathbf{A}_{22}}{\mathbf{A}_{11} + \mathbf{A}_{12}/Z_0 + \mathbf{A}_{21}Z_0 + \mathbf{A}_{22}}, \tag{5.13}$$

$$\mathbf{S}_{12} = \frac{2\det(\mathbf{A})}{\mathbf{A}_{11} + \mathbf{A}_{12}/Z_0 + \mathbf{A}_{21}Z_0 + \mathbf{A}_{22}}, \tag{5.14}$$

$$\mathbf{S}_{21} = \frac{2}{\mathbf{A}_{11} + \mathbf{A}_{12}/Z_0 + \mathbf{A}_{21}Z_0 + \mathbf{A}_{22}}, \tag{5.15}$$

$$\mathbf{S}_{22} = \frac{-\mathbf{A}_{11} + \mathbf{A}_{12}/Z_0 - \mathbf{A}_{21}Z_0 + \mathbf{A}_{22}}{\mathbf{A}_{11} + \mathbf{A}_{12}/Z_0 + \mathbf{A}_{21}Z_0 + \mathbf{A}_{22}}. \tag{5.16}$$

Identification of the different resonances

The magnitude $\mathbf{S}_{12}$ with respect to the frequency ν shows three different types of resonances.

1. The resonator on the PCB without shunting or bridging series resonant circuits produces the characteristic curve in figure 5.3. The peaks reach $0\,\mathrm{dB}$ if the transmission line is lossless, i.e. the attenuation constant α is zero. Figure 5.3 is plotted for a lossy transmission line. As expected the resonance frequencies depend on the resonator length l. However it depends also on the coupling capacitances C_{c}. Numerical computations show that the resonance frequencies increase if the capacitances are reduced and vice versa.

2. The bridging series resonant circuits create peaks and dips between the resonator resonances (figure 5.4). They either start with a peak followed by a dip or vice versa. The order of the peak and the dip alternate from resonator resonance to resonator resonance.

3. The shunting series resonant circuits show a similar behaviour like the bridging ones (figure 5.5). However they differ in the order of the peak and the dip.

The model describes the magnitude $\mathbf{S}_{12}$ of the resonator qualitatively. But it does not fit the measured curve perfectly. The reasons are the following.

- The model has several free parameters and it is difficult to choose good initial values for the non-linear fit. However it is possible to adjust them by hand such that parts of the curve match.

- The different shunting and bridging resonances influence each other and shift the resonator resonance frequencies. The influence increases for larger capacitances of the series resonant circuits. It is therefore possible that sample holder resonances which can not be resolved with the network analyzer impact the curve.

- The model assumes that the sample holder resonances are excited at specific positions on the transmission line (figure 5.2). In reality the resonances are excited along the whole transmission line.

Figure 5.6 shows the measured magnitude $\mathbf{S}_{12}$ of PCB in figure 4.2a and a model fit. The fit parameters listed in the figure caption were found manually.

A possible refinement of the model is sketched in section 6.2.

5.2.2. Measured resonator resonances

The resonator resonances can be fitted by the Lorentzian function

$$S(\nu) = a + \frac{b}{\sqrt{1 + 4Q^2(1 - \nu/\nu_0)^2}}, \tag{5.17}$$
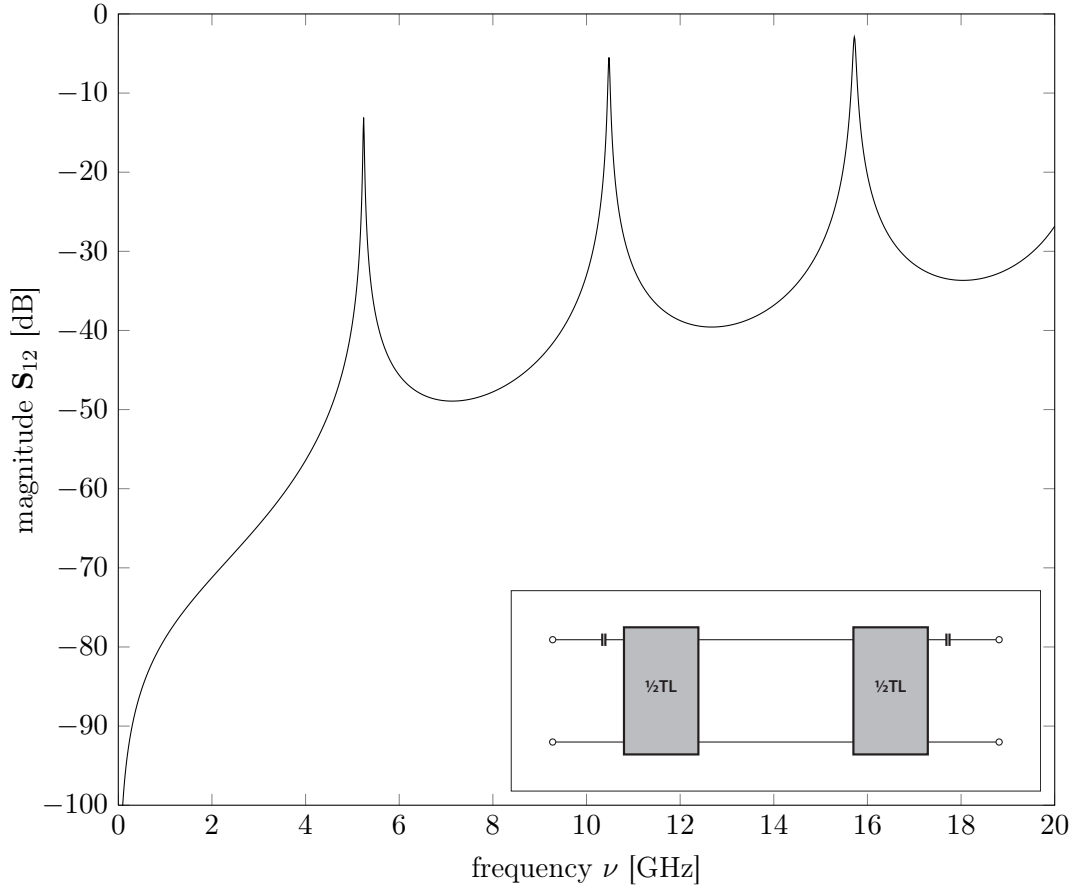
Figure 5.3.: Magnitude $\mathbf{S}_{12}$ of the model shown in the inset. It reflects the qualitative behavior of a resonator on PCB shown in figure 4.2a.

S parameter	T [K]	a	b	ν_0 [GHz]	Q
$\mathbf{S}_{12}$	77	5.50×10^{-4}	1.25×10^{-1}	4.893	116.8
$\mathbf{S}_{12}$	77	-1.27×10^{-3}	2.99×10^{-1}	10.009	112.6
$\mathbf{S}_{12}$	77	8.06×10^{-3}	3.45×10^{-1}	15.091	127.1
$\mathbf{S}_{34}$	77	4.99×10^{-4}	1.12×10^{-1}	5.409	124.2
$\mathbf{S}_{34}$	77	-2.17×10^{-3}	2.49×10^{-1}	10.135	115.0
$\mathbf{S}_{34}$	77	2.49×10^{-2}	4.08×10^{-1}	15.712	126.8
$\mathbf{S}_{12}$	300	-4.50×10^{-3}	7.21×10^{-2}	5.239	62.7
$\mathbf{S}_{12}$	300	-2.06×10^{-3}	1.60×10^{-1}	10.720	76.3
$\mathbf{S}_{12}$	300	4.98×10^{-3}	1.99×10^{-1}	16.163	84.5
$\mathbf{S}_{34}$	300	2.74×10^{-4}	6.06×10^{-2}	5.784	70.9
$\mathbf{S}_{34}$	300	-2.05×10^{-3}	1.30×10^{-1}	10.861	75.7
$\mathbf{S}_{34}$	300	1.65×10^{-2}	2.47×10^{-1}	16.831	79.4

Table 5.1.: The fit parameters of the resonator resonances
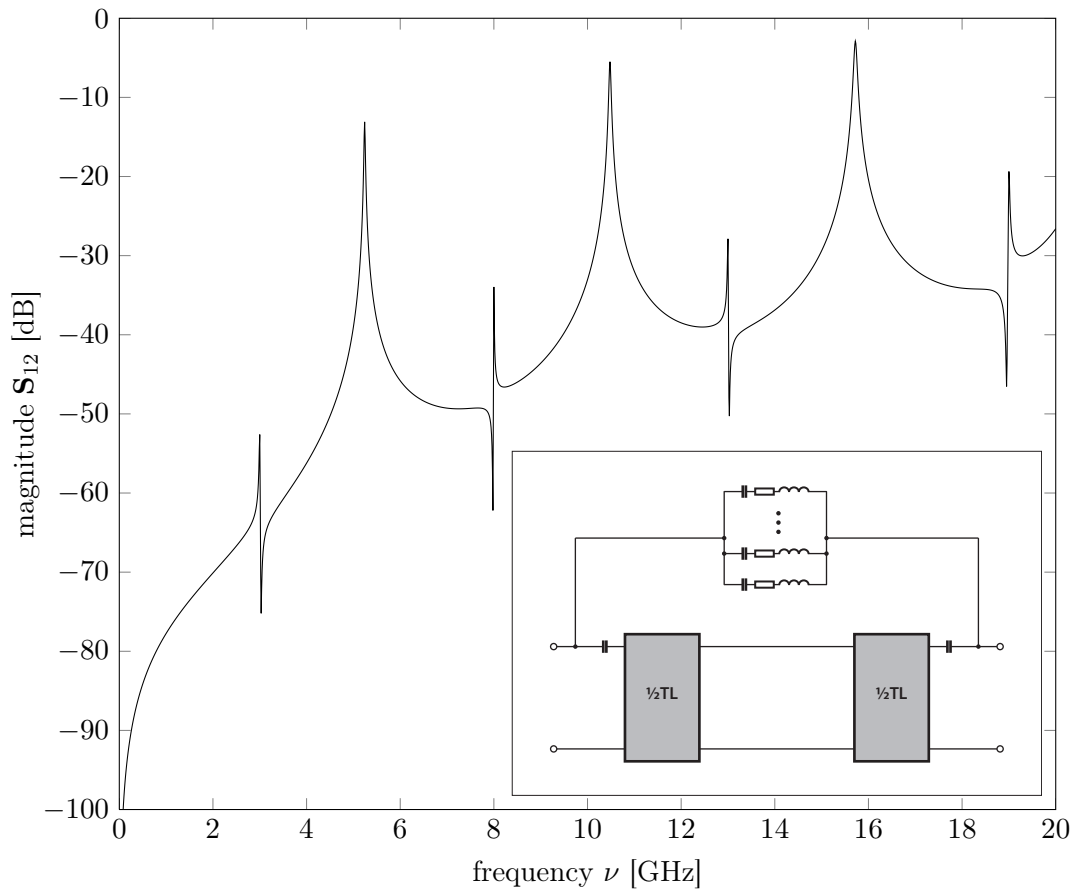
Figure 5.4.: Magnitude $\mathbf{S}_{12}$ of the model shown in the inset. The bridging series resonant circuits create peaks and dips between the resonator resonances. The order of the peak and the dip alternates from resonator resonance to resonator resonance.
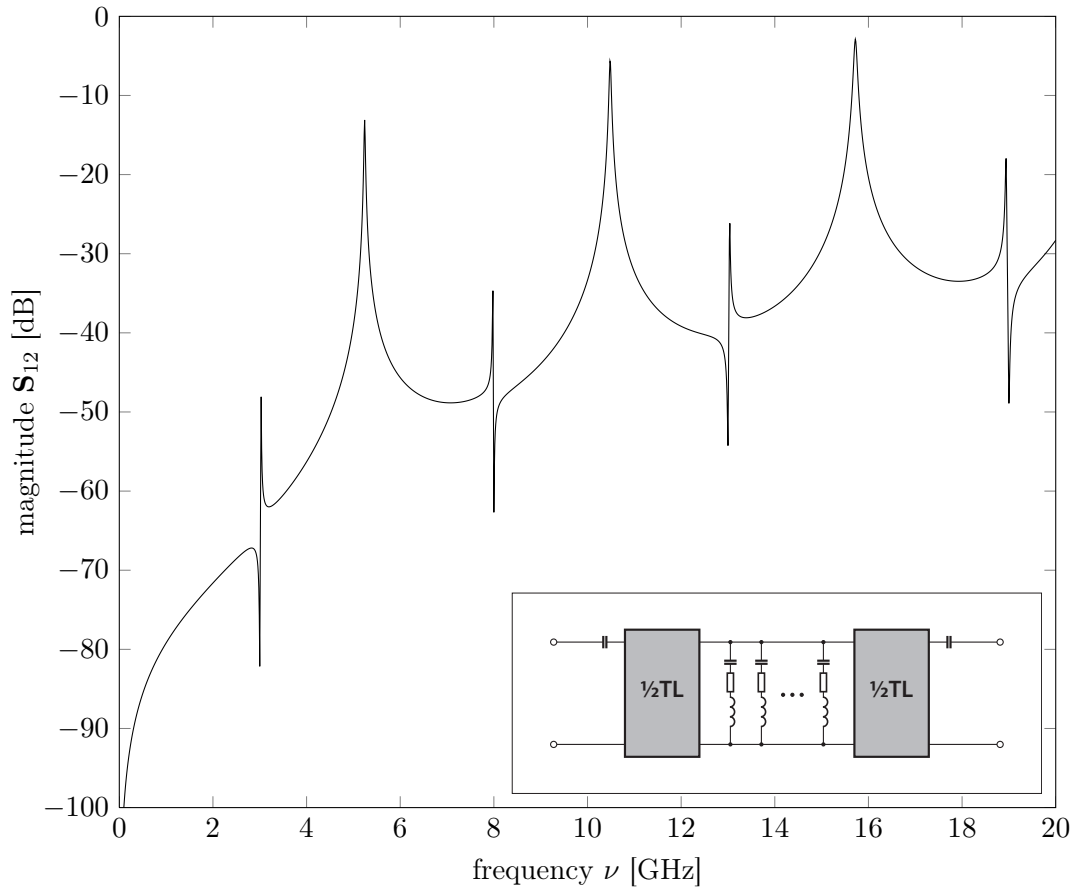
Figure 5.5.: Magnitude $\mathbf{S}_{12}$ of the model shown in the inset. The shunting series resonant circuits show the same behavior as the bridging series resonant circuits. They only differ in the order of the peak and the dip.
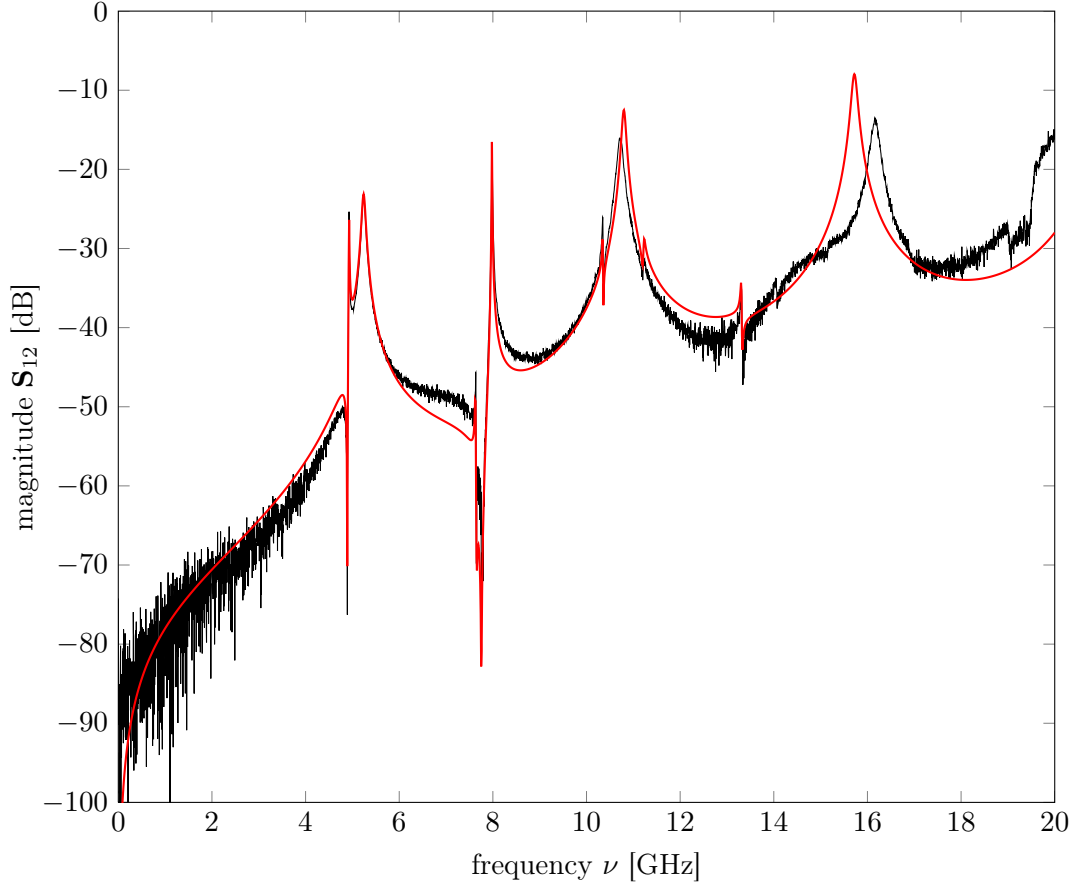
Figure 5.6.: Model fit of magnitude $\mathbf{S}_{12}$ of PCB shown in figure 4.2a at 300 K. Fit parameters are: $C_\mathrm{c} = 18\,\mathrm{fF}$, $\alpha = 1.9\,\mathrm{m}^{-1}$, $v_\mathrm{ph} = 1.31 \times 10^8\,\mathrm{m\,s}^{-1}$ respectively $\epsilon_\mathrm{eff} = 5.2$, $l = 12.3\,\mathrm{mm}$; Bridging resonance circuits (ν_s, C, Q): (7.980 GHz, 35 aF, 1000), (13.31 GHz, 2.5 aF, 600); Shunting resonance circuits (ν_s, C, Q): (4.89 GHz, 210 fF, 2000), (7.637 GHz, 2.5 fF, 500), (10.355 GHz, 110 aF, 1000), (11.21 GHz, 120 aF, 300)

where Q is the quality factor of the resonance and ν_0 is the resonance frequency. The parameters a and b are just an offset respectively a scaling factor. [3]

The fitted parameters are listed in table 5.1. The measured resonance frequencies are close to the expected values calculated in section 2.3.2.

The numbers show the following.

1. The resonance frequencies differ between the two resonators even for same temperatures and although the resonators are of equal lengths.

2. If the temperature is lowered the resonance frequencies decrease and the quality factors increase.

That can probably be explained as follows.

1. The bends of transmission lines at the entry and exit of the resonators 12 and 34 differ (figure 4.2a). Therefore they couple differently to the resonator. This could result in different resonance frequencies.

2. If the temperature is lowered the resistance of the conductors decreases. Therefore the resonances become sharper and the quality factors increase. In the dielectric the thermal motion decreases and the dipole moments can be aligned more easily. This means that the relative dielectric constant of the dielectic increases and therefore also the effective dielectric constant. The resonance frequency becomes lower (see formulas (2.3) and (2.4)).

5.2.3. Measured sample holder resonances

The sample holder resonances are either of the form dip-peak or peak-dip. They can be described by the frequency ν_d of the dip and the frequency ν_p of the peak and the values of the S-parameter $S(\nu_d)$ and $S(\nu_p)$ at those frequencies. The values are summarized in table 5.2.

5.3. Analysis of the PCBs with throughs

The two PCBs with throughs shown in figure 4.2b and 4.2c are measured at room temperature and in liquid nitrogen. Suppose we send a microwave signal in at port 2 and measure the transmission, the reflection and the crosstalk. The S parameters $\mathbf{S}_{12}$, $\mathbf{S}_{22}$, $\mathbf{S}_{32}$ and $\mathbf{S}_{42}$ quantify these parts. Figures 5.7, 5.8, 5.9 and 5.10 show the S-parameters for the two PCBs.

In the following the data is discussed.

- The magnitude of $\mathbf{S}_{12}$ becomes positive above about $16\,\mathrm{GHz}$. The effect does not depend on temperature nor the PCB. As a passive element the PCB can not amplify the transmitted signal. Maybe an error was made during measuring the dipstick cables. In chapter 5.1 the dipstick cables are de-embedded assuming that the crosstalk among them is negligible. Perhaps this assumption does not hold above $16\,\mathrm{GHz}$. Further investigations are required to fix the problem.

S parameter	T [K]	Resonance type	ν_d [GHz]	$S(\nu_d)$ [dB]	ν_p [GHz]	$S(\nu_p)$ [dB]
$\mathbf{S}_{12}$	77	dip-peak	4.002	-81.21	4.131	-25.66
$\mathbf{S}_{12}$	77	peak-dip	6.421	-51.20	6.395	-46.49
$\mathbf{S}_{12}$	77	dip-peak	6.597	-66.13	6.682	-24.57
$\mathbf{S}_{12}$	77	peak-dip	8.723	-53.30	8.657	-33.39
$\mathbf{S}_{12}$	77	peak-dip	9.510	-35.94	9.449	-29.56
$\mathbf{S}_{12}$	77	dip-peak	12.700	-40.70	12.780	-35.77
$\mathbf{S}_{12}$	77	peak-dip	13.030	-37.78	12.970	-33.91
$\mathbf{S}_{12}$	77	dip-peak	16.440	-36.83	16.740	-28.73
$\mathbf{S}_{12}$	77	peak-dip	17.290	-30.79	17.120	-27.10
$\mathbf{S}_{12}$	77	dip-peak	17.840	-26.96	17.940	-23.03
$\mathbf{S}_{12}$	77	peak-dip	18.600	-24.39	18.540	-22.70
$\mathbf{S}_{34}$	77	dip-peak	3.920	-93.83	4.131	-29.20
$\mathbf{S}_{34}$	77	only peak			6.400	-22.34
$\mathbf{S}_{34}$	77	dip-peak	6.416	-30.12	6.421	-28.75
$\mathbf{S}_{34}$	77	only peak			6.682	-30.68
$\mathbf{S}_{34}$	77	peak-dip	8.684	-55.80	8.653	-43.07
$\mathbf{S}_{34}$	77	dip-peak	11.550	-47.43	11.580	-38.84
$\mathbf{S}_{34}$	77	peak-dip	13.020	-50.32	12.970	-39.62
$\mathbf{S}_{34}$	77	dip-peak	17.410	-32.66	17.540	-23.81
$\mathbf{S}_{34}$	77	dip-peak	17.860	-29.55	17.950	-25.96
$\mathbf{S}_{34}$	77	dip-peak	18.340	-30.94	18.400	-27.19
$\mathbf{S}_{34}$	77	peak-dip	18.650	-39.66	18.540	-23.24
$\mathbf{S}_{34}$	77	dip-peak	19.110	-34.09	19.160	-28.17
$\mathbf{S}_{12}$	300	dip-peak	4.891	-75.71	4.928	-25.42
$\mathbf{S}_{12}$	300	peak-dip	7.650	-69.31	7.635	-45.35
$\mathbf{S}_{12}$	300	dip-peak	7.770	-90.08	7.983	-18.01
$\mathbf{S}_{12}$	300	peak-dip	10.360	-34.55	10.350	-25.73
$\mathbf{S}_{12}$	300	dip-peak	11.200	-33.90	11.230	-31.07
$\mathbf{S}_{12}$	300	peak-dip	13.340	-46.34	13.310	-34.94
$\mathbf{S}_{12}$	300	peak-dip	14.080	-36.88	14.040	-33.47
$\mathbf{S}_{12}$	300	dip-peak	15.150	-31.19	15.180	-28.74
$\mathbf{S}_{12}$	300	peak-dip	19.070	-30.84	18.970	-26.83
$\mathbf{S}_{34}$	300	dip-peak	4.747	-76.42	4.928	-23.39
$\mathbf{S}_{34}$	300	only peak			7.637	-16.64
$\mathbf{S}_{34}$	300	only peak			7.983	-30.15
$\mathbf{S}_{34}$	300	dip-peak	10.270	-42.98	10.290	-32.17
$\mathbf{S}_{34}$	300	peak-dip	10.360	-38.92	10.350	-31.29
$\mathbf{S}_{34}$	300	peak-dip	13.340	-52.40	13.310	-38.07
$\mathbf{S}_{34}$	300	dip-peak	13.760	-52.59	13.780	-34.54
$\mathbf{S}_{34}$	300	peak-dip	15.470	-44.24	15.430	-32.48

Table 5.2.: The sample holder resonances

Figure 5.7.: Magnitude of S-parameters of PCB shown in figure 4.2b at 77 K.

Figure 5.8.: Magnitude of S-parameters of PCB shown in figure 4.2b at 300 K.
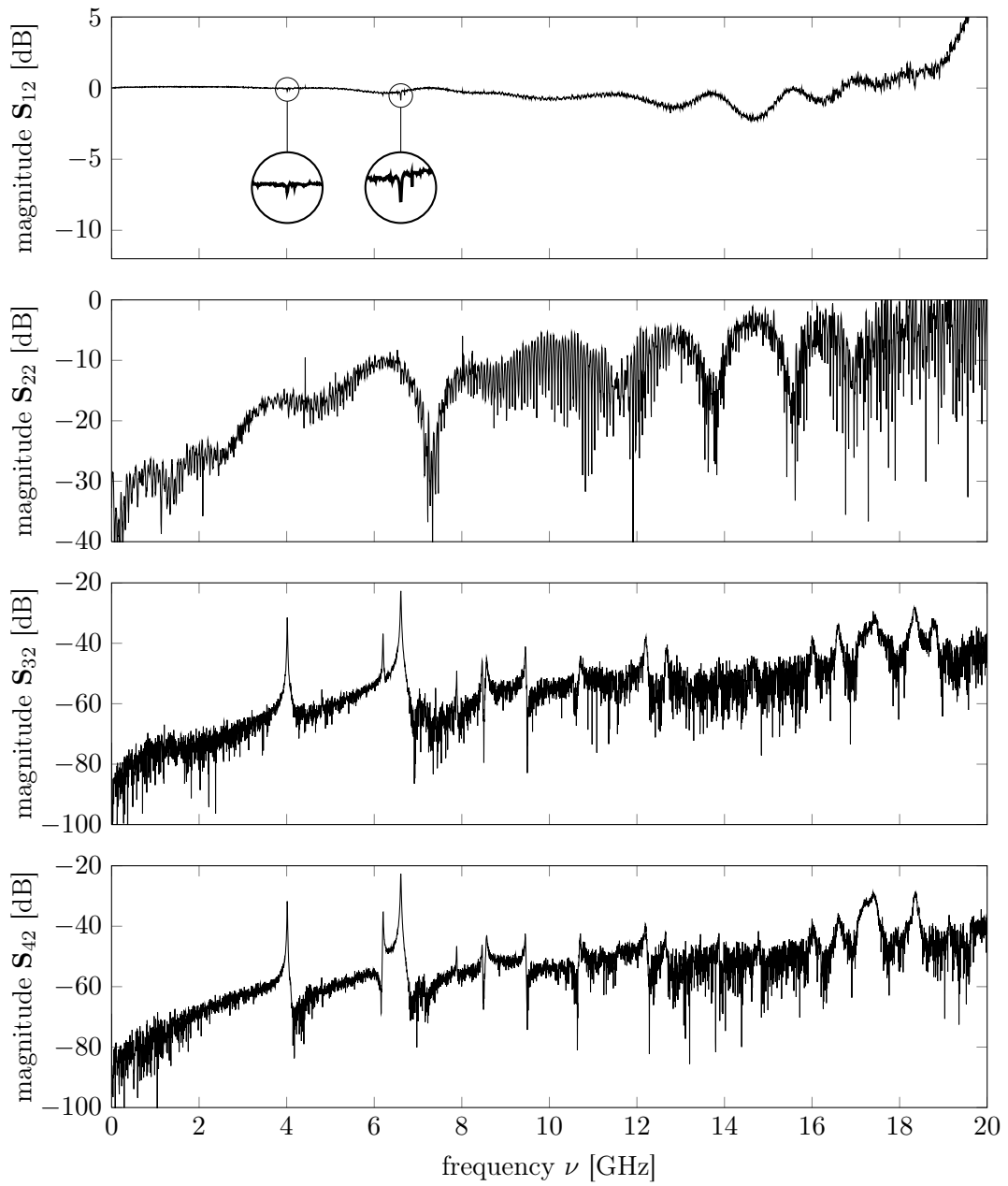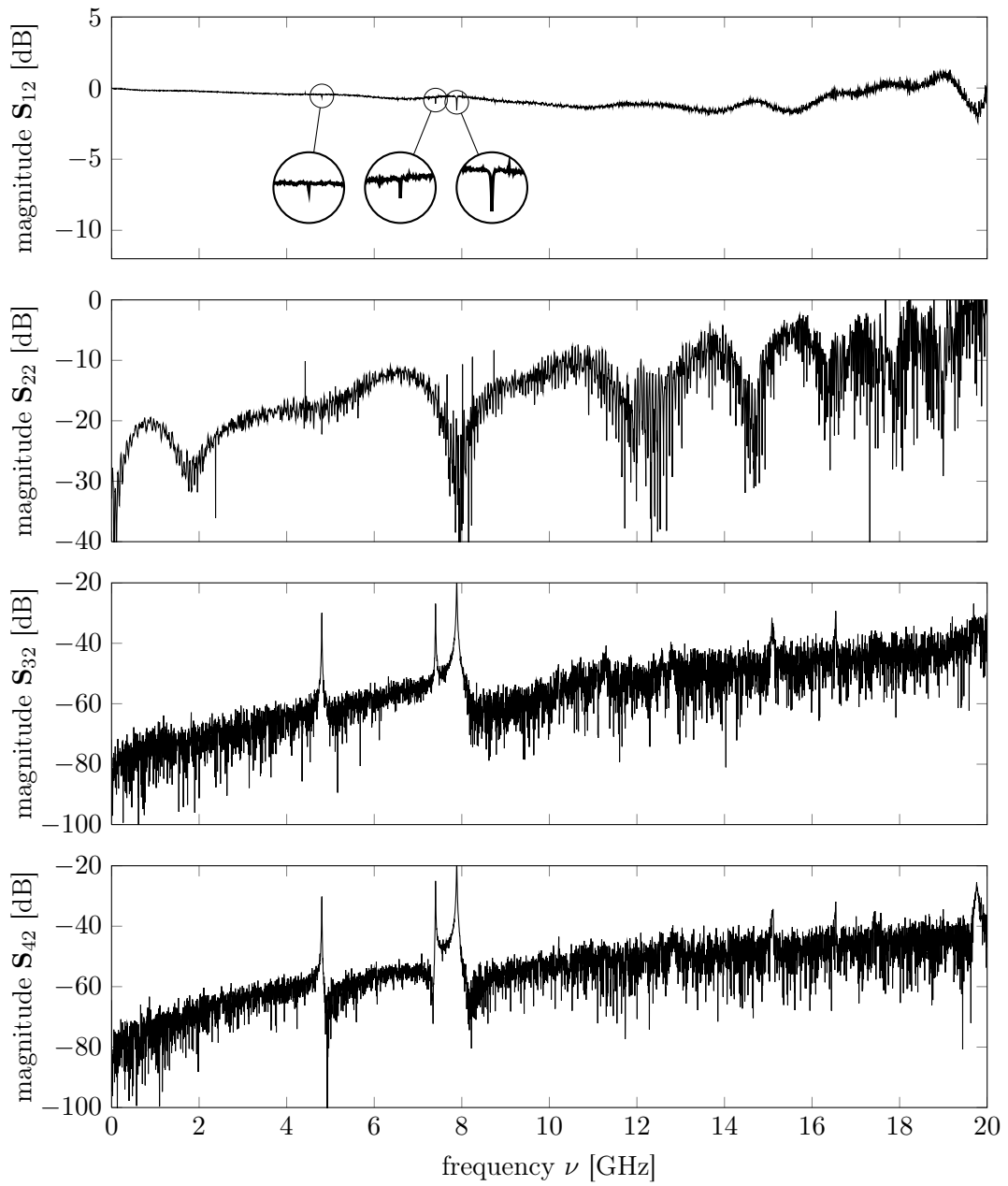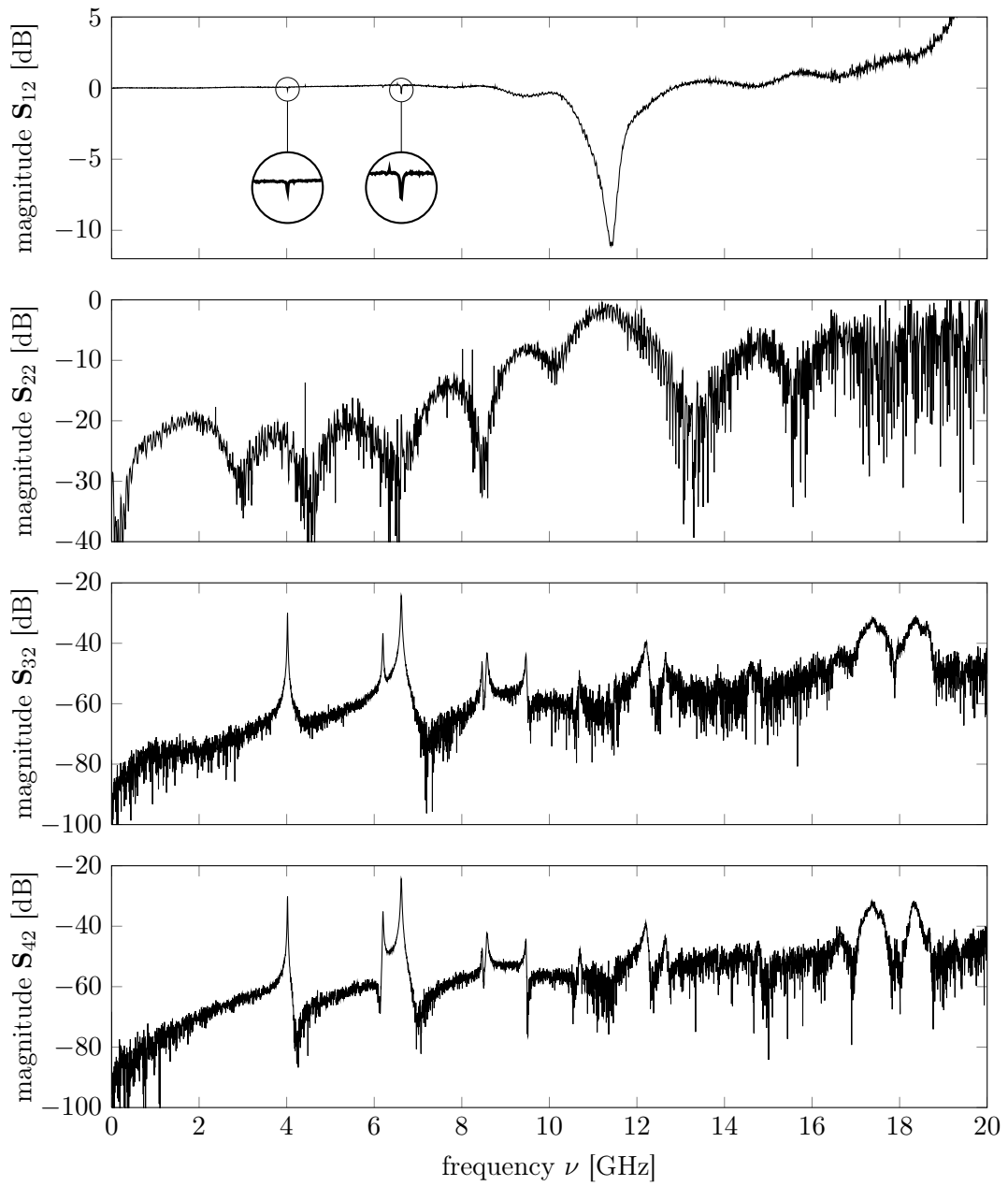
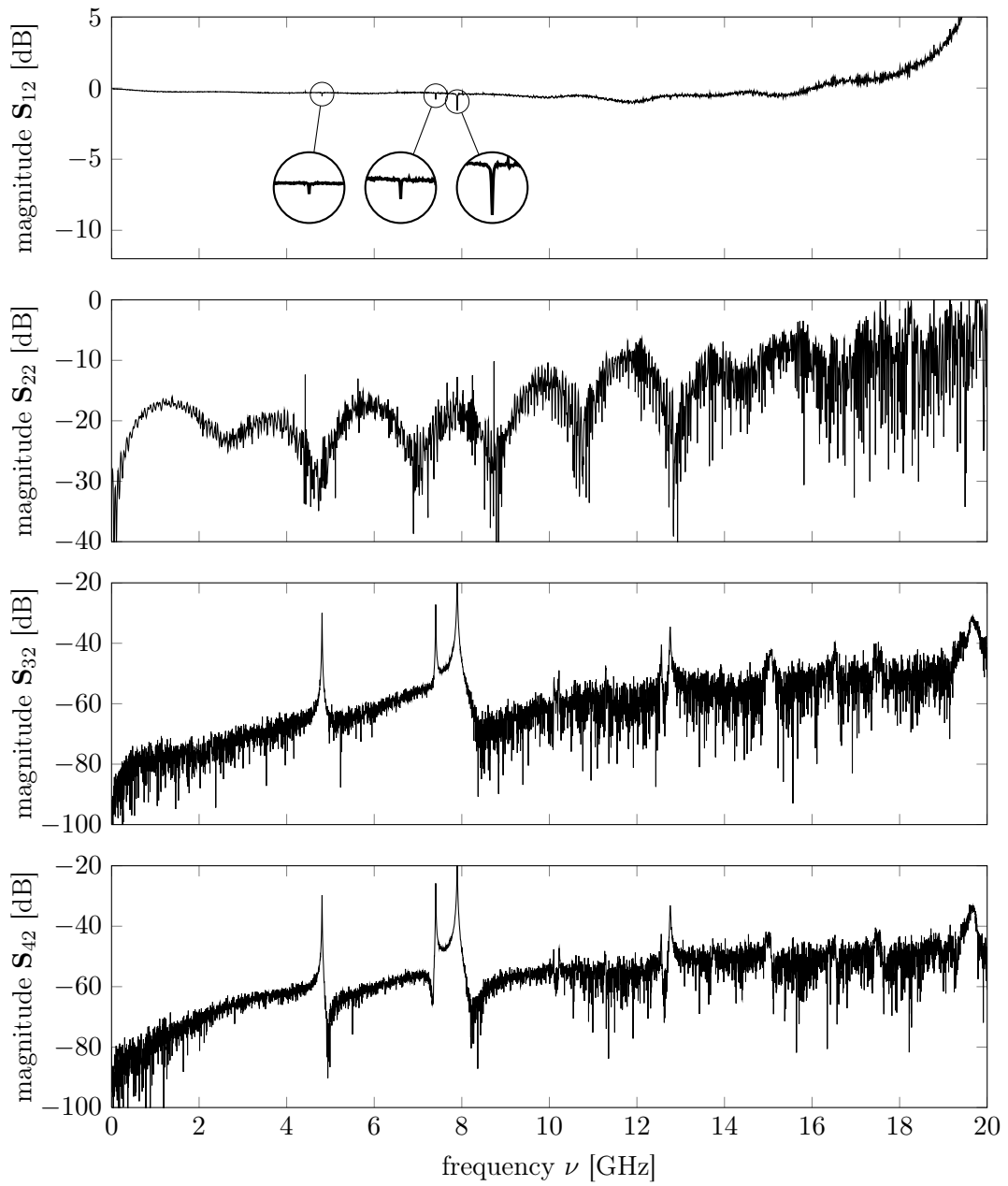Figure 5.9.: Magnitude of S-parameters of PCB shown in figure 4.2c at 77 K.

Figure 5.10.: Magnitude of S-parameters of PCB shown in figure 4.2c at 300 K.

PCB	T [K]	ν_0 [GHz]
contour vias	77	4.019
contour vias	77	6.618
area vias	77	4.013
area vias	77	6.607
contour vias	300	4.808
contour vias	300	7.404
contour vias	300	7.896
area vias	300	4.803
area vias	300	7.400
area vias	300	7.884

Table 5.3.: Resonances in $\mathbf{S}_{12}$ for PCBs with throughs

- In all measurements the parameter $\mathbf{S}_{12}$ shows dips at certain frequencies. They coincidence with peaks in $\mathbf{S}_{32}$ and $\mathbf{S}_{42}$ which means that the crosstalk is large. Table 5.3 lists those frequencies. It indicates that the influence of the area vias is insignificant. Therefore it is likely that the crosstalk is mediated via the sample holder.

- The huge dip in $\mathbf{S}_{12}$ in figure 5.9 occurs at a frequency of 11.420 GHz. At this frequency the crosstalk is low since the value of $\mathbf{S}_{32}$ and $\mathbf{S}_{42}$ is around -60 dB. However the dip stems from reflections at port 2 (see $\mathbf{S}_{22}$ in figure 5.9). At room temperature the same PCB do not show the huge dip in $\mathbf{S}_{12}$. It is possible that the connector at port 2 or other connectors of the dipstick cables are badly soldered. At low temperatures connector pins are contracted and the contacts could become bad. The wave is reflected. Rosenberger only guarantees a good performance for the connector 19S102-40ML5 in the temperature range from $-65\,°\mathrm{C}$ to $155\,°\mathrm{C}$ [5].

5.3.1. Effects of the area vias

In order to study the influence of the area vias we compare the transmission $\mathbf{S}_{12}$ of the PCB with and without them. The goal is to achieve a high transmission and a low crosstalk over a wide frequency range.

At room temperature the transmission is very similar for the PCB with and without area vias. It even begins to wiggle for lower frequencies with area vias. The same is true in liquid nitrogen apart from the huge dip in the transmission in the diagram 5.9. This dip probably comes from reflections at the connector and not from the lack of area vias. This suggests the assumption that the area vias are not needed for a good transmission. However further measurements are needed to confirm this since the transmission of the PCB without area vias shows a huge dip.

Also the crosstalk is very similar for the both PCBs. It is always around -50 dB apart from the resonances.

6. Prospect

This chapter presents further investigations and improvements.

6.1. Alternative algorithms for area via placement

Alternative methods to place area vias are methods to tessellate a subspace of the plane. A group of algorithms is presented in [4]. They can solve problems as described in the following example.

Suppose a company wants to place N letter-boxes in a town. The goal is that the distance to the next letter-box is minimal for each inhabitant. To optimize the distribution of the boxes we know the population density of the town. [4, page 5]

6.2. Resonance model

The resonance model presented in section 5.2.1 assumes that the sample holder resonances are only excited at two positions along the transmission line on the PCB. But in reality the transmission line excite them continuously. This can be taken into account with the extended circuit in figure 6.1.
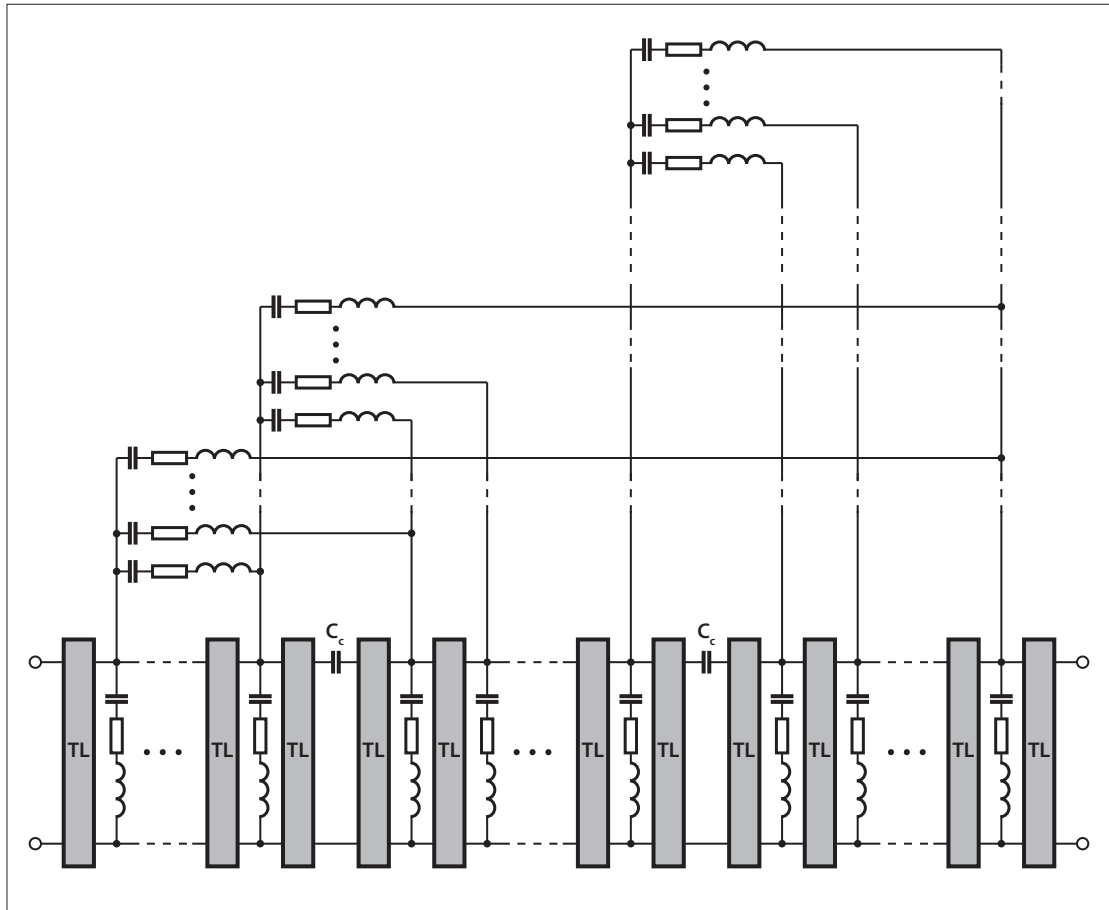
Figure 6.1.: Refined resonance model

7. Acknowledgements

This semester thesis offered me insights in several aspects. I gained knowledge in microwave technologies, four port networks and in several CAD programs and Mathematica. I thank *Prof. Andreas Wallraff* who gave me the opportunity for this work. My advisor *Matthias Baur* guided and encouraged me during the work. I thank him for his advice and support. *Johannes Fink* designed the PCBs with throughs and resonators. For that I express him my gratitude.

Bibliography

[1] Arlon-Microwave Materials: *AD1000*, 2.1 edition, 2012.

[2] Fink, J.: *Quantum nonlinearities in strong coupling circuit QED*. PhD thesis, Swiss Federal Institute of Technology Zurich, 2010.

[3] Petersan, P. J. and Anlage, S. M.: *Measurement of resonant frequency and quality factor of microwave resonators: Comparison of methods*. Journal of Applied Physics, 84(6):3392–3402, 1998.

[4] Raskob, C.: *Schwerpunkt-Voronoi-Diagramme*. Diplomarbeit, FernUniversität in Hagen, 2004.

[5] Rosenberger Hochfrequenztechnik GmbH: *Technical data sheet SMP 19S102-40ML5*. `http://rosenberger.shopwiesel.de/images/documents/db/19S102-40ML5.pdf`, 2012.

[6] Schmidlin, S.: *Design and characterization of microwave printed Circuit Boards for circuit QED experiments*. Semester thesis, 2008.

[7] Simons, R. N.: *Coplanar waveguide circuits, components, and systems*. Wiley-Interscience, 2001.

[8] Wolff, I.: *Coplanar Microwave Integrated Circuits*. Wiley-Interscience, 2006.

[9] Yu, M., Vahldieck, R., and Huang, J.: *Comparing coax launcher and wafer probe excitation for 10 mil conductor backed CPW with via holes and airbridges*. In *Microwave Symposium Digest, 1993., IEEE MTT-S International*, pages 705 –708 vol.2, 1993.

A. User manual for the impatiens algorithm

The AutoLISP routines and the Octave functions are contained on the attached CD. The following steps show how the area vias are placed.

Export the polygon P and the positions of the contour vias V

1. Load all AutoLISP routines.

2. Launch the following command to export the polygon P.
   `(writeCoordinates "path\\polygon.txt" (getPolyline))`

3. Launch the following command to export the set V.
   `(writeCoordinates "path\\contour vias.txt" (getPolyline))`

Position the area vias

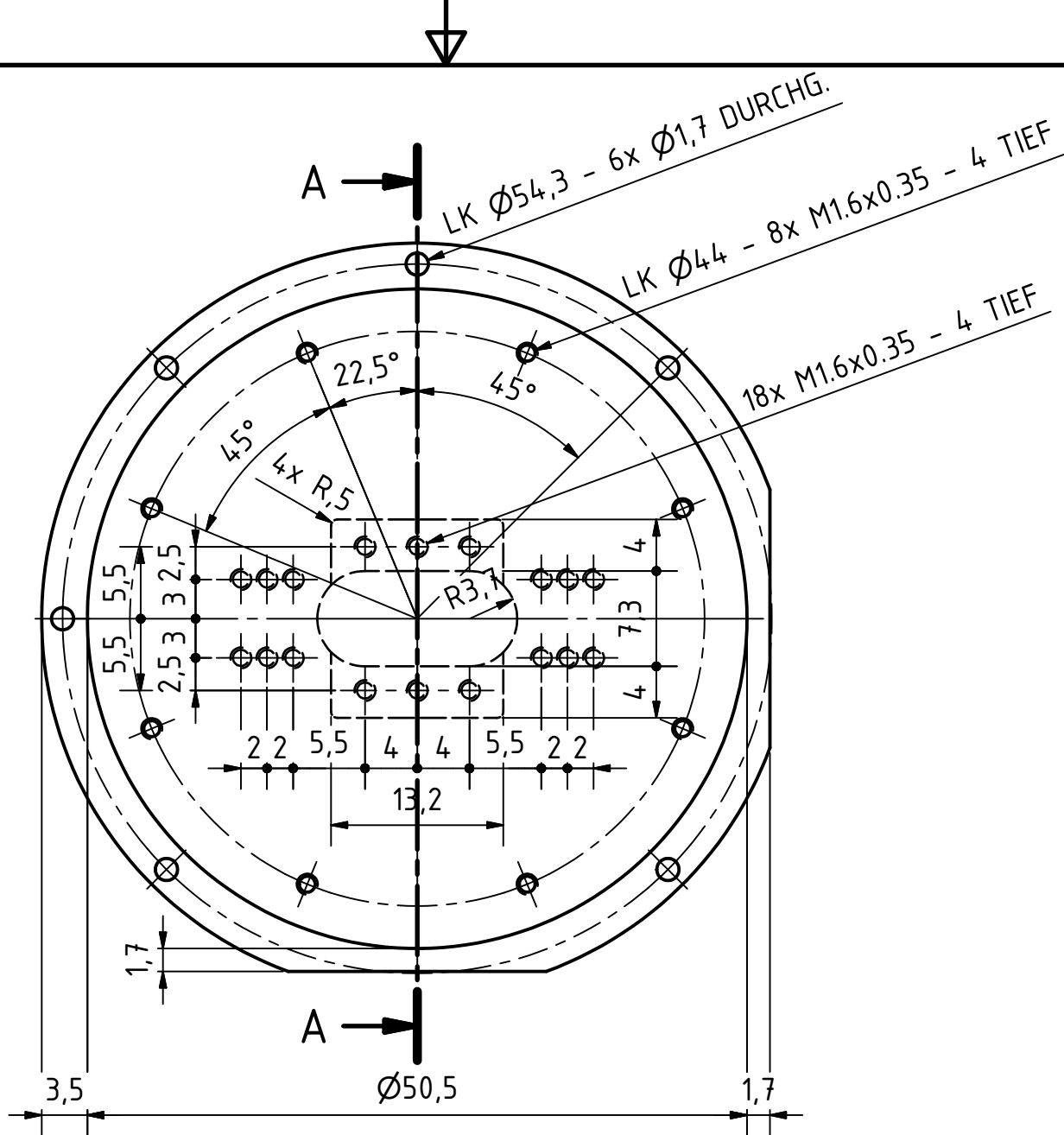Launch the following command in Octave.
`main("path/polygon.txt", "path/contour vias.txt",`
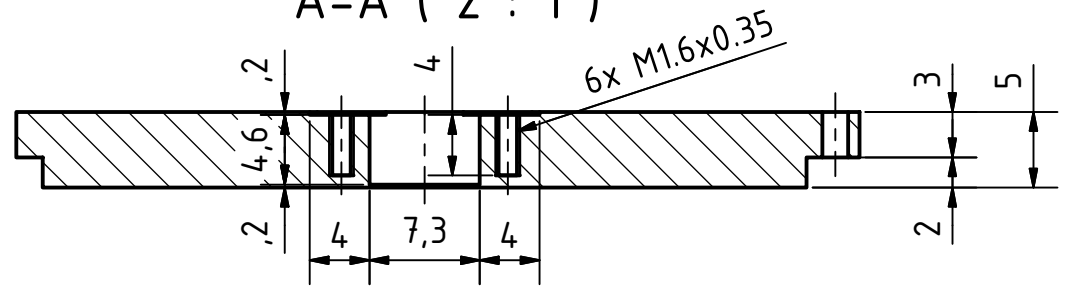`"path/area vias.txt", minSpace, maxSpace)`

Draw the area vias

Launch the following command in AutoCAD 2011 to draw the area vias.
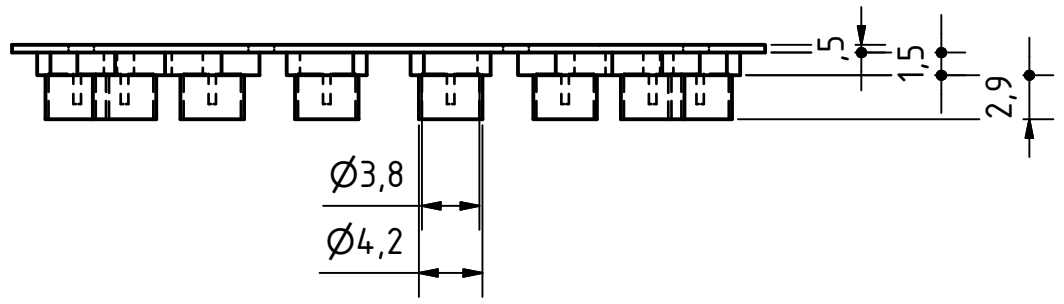`(drawVias (readCoordinates "path\\area vias.txt") radius)`

B. Sample holder

LK Ø54,3 – 6x Ø1,7 DURCHG.

LK Ø44 – 8x M1.6x0.35 – 4 TIEF

18x M1.6x0.35 – 4 TIEF

A

A

22,5°

45°

45°

4x R,5

R3,1

5,5 5,5

2,5 3 3 2,5

5,5 5,5

2,5 3

4

7 3

4

2 2 5,5 4 4 5,5 2 2

13,2

1,7

3,5 Ø50,5 1,7

A–A (2 : 1)

,2

4,6

,2

4 7,3 4

6x M1.6x0.35

3 5

2

				Datum	Name	Massstab 2:1	5x
			Gezeichnet	06.05.2011	Samuel H.	Sauerstofffreies Kupfer	
			Kontrolliert			Sampleholder with coils	
			Norm				
						Mount	1
							A4
Status	Änderungen	Datum	Name				

8x Ø1,7 DURCHG.

□4,5

LK Ø44
LK Ø42

45°

22,5°

,5

1,5

2,9

Ø3,8
Ø4,2

				Massstab 2:1		
			Datum	Name		
			Gezeichnet	06.05.2011	Samuel H.	Sampleholder with coils
			Kontrolliert			
			Norm			
						PCB
Status	Änderungen	Datum	Name			2 / A4

LK Ø42

LK Ø54,3 – 6x M1.6x0.35 – 7 TIEF

B

B

45°

45°

M3x0.5 – 4 TIEF

22,5°

1,5

Ø49

1,5

Ø51

3,3

B–B (2 : 1)

Ø6,1

Ø5,1

3,8

M3x0.5

4

4,8

1,7

2,6

					Massstab 2:1	5x
					Sauerstofffreies Kupfer	
				Datum	Name	
			Gezeichnet	06.05.2011	Samuel H.	
			Kontrolliert			Sampleholder with coils
			Norm			
					Lid	3
						A4
Status	Änderungen	Datum	Name			

7,00

0,20

0,20

R0,10

4,40

3,00

4,00

0,50

R0,50

R0,50

R3,50

R0,80

5,00

4,00

5,50

7,50
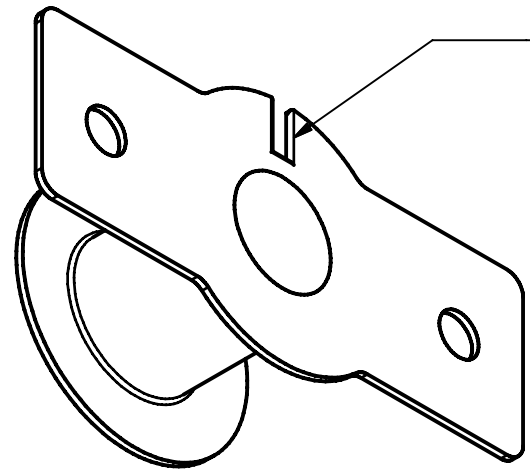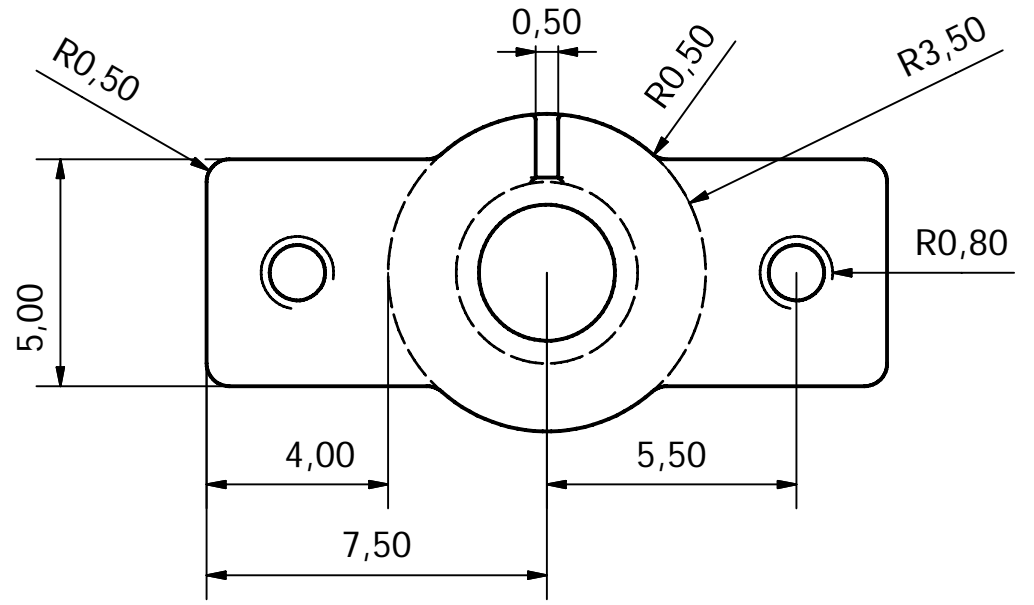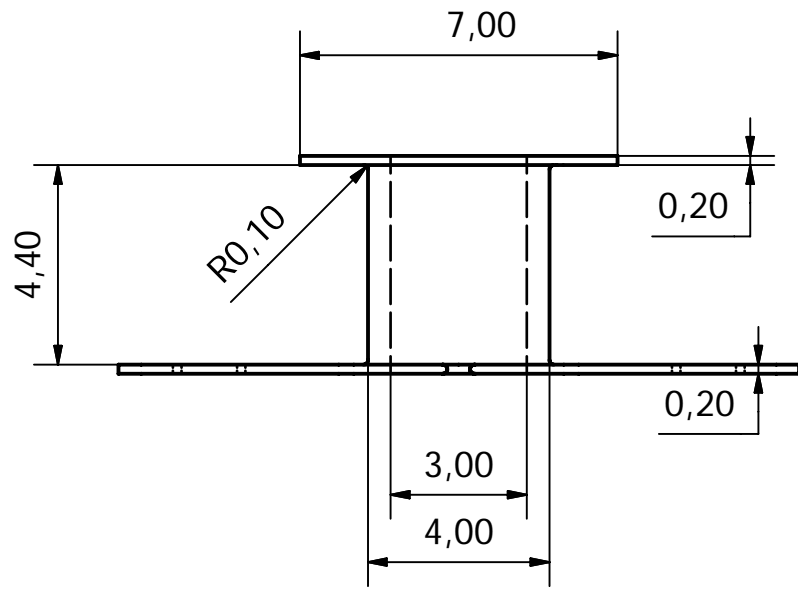
Kanten so rund wie Möglich

Designed by	Checked by	Approved by	Date		Date	
Romeo Bianchetti					20.06.2006	

Oxigen Free Copper

3x

Coil holder

Edition

Sheet
1 / 1

R0,80

0,50

Ø11,00

R9,00

Ø12,00

10,00

13,50

11,50

6,00

18,00

11,00

0,50

4,00

12,00

0,20
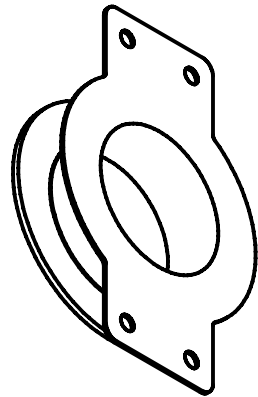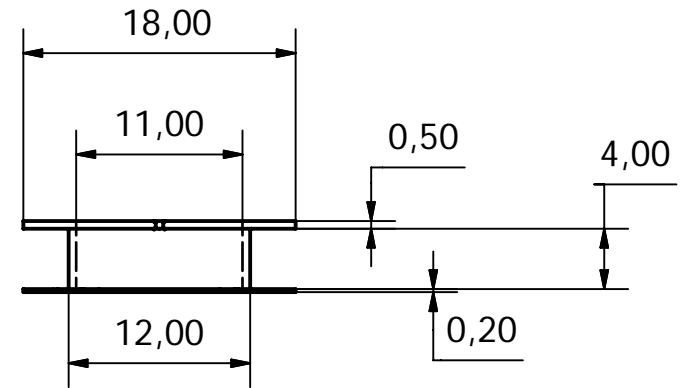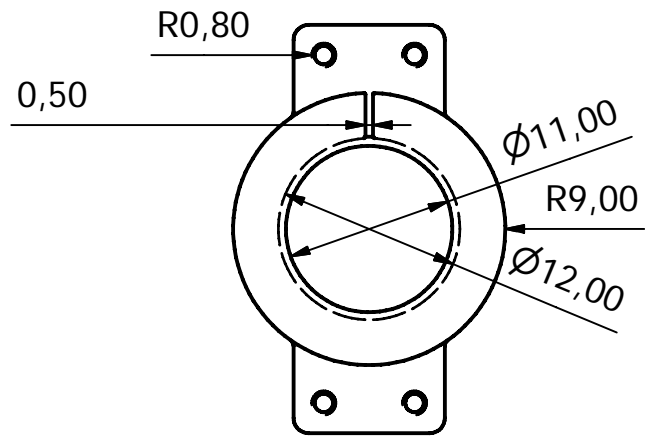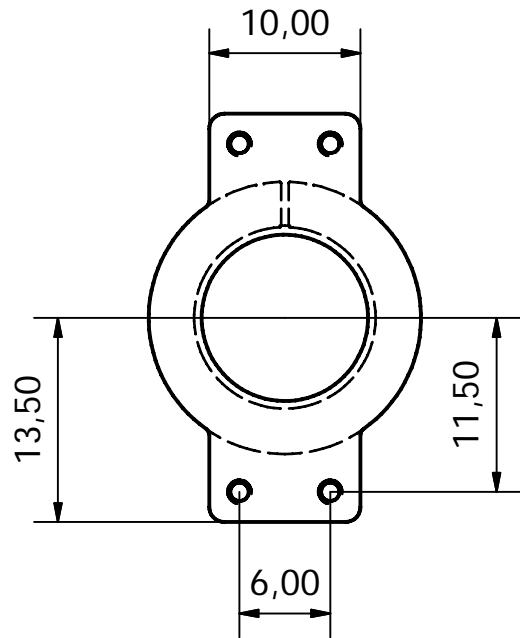
Designed by	Checked by	Approved by	Date		Date	
Romeo Bianchetti					21.06.2006	

<table>
<tr><td rowspan="2">2x</td><td colspan="3">Oxygen Free Copper</td></tr>
<tr><td>Coil holder big</td><td>Edition
1.0</td><td>Sheet
1 / 1</td></tr>
</table>

C. De-embedding the coaxial cables

Figure C.1 shows the general situation. The yellow network has n ports. Each port is connected with a coaxial cable symbolized by blue rectangles. The following S-matrices are known.

- The S-matrix of the green n port network is $\mathbf{S}^{\mathrm{m}}$.

- The S-matrices of the blue two port networks are $\mathbf{C}^{(i)}$ where i runs from one to n.

The S-matrix $\mathbf{S}^{\mathrm{d}}$ of the yellow n port is unknown. It should be expressed with the known matrices.

The green n port network gives the following relations between the incident power waves A_i and the reflected power waves B_i

$$B_i = \sum_{j=1}^{n} \mathbf{S}_{ij}^{\mathrm{m}} A_j. \tag{C.1}$$

Each blue two port network gives analogously

$$B_i = \mathbf{C}_{11}^{(i)} A_i + \mathbf{C}_{12}^{(i)} b_i, \tag{C.2}$$

$$a_i = \mathbf{C}_{21}^{(i)} A_i + \mathbf{C}_{22}^{(i)} b_i. \tag{C.3}$$

The unknown yellow n port network states

$$b_i = \sum_{j=1}^{n} \mathbf{S}_{ij}^{\mathrm{d}} a_j. \tag{C.4}$$

Equations (C.2) and (C.3) can be rewritten. The first formula can be solved for b_i if we assume that $\mathbf{C}_{12}^{(i)}$ is unequal to zero for all i. Plugging the obtained expression into formula (C.3) yields

$$b_i = \frac{B_i - \mathbf{C}_{11}^{(i)} A_i}{\mathbf{C}_{12}^{(i)}}, \tag{C.5}$$

$$a_i = -\frac{\det(\mathbf{C}^{(i)})}{\mathbf{C}_{12}^{(i)}} A_i + \frac{\mathbf{C}_{22}^{(i)}}{\mathbf{C}_{12}^{(i)}} B_i. \tag{C.6}$$

Inserting these two expressions into equation (C.4), we obtain

$$\frac{B_i - \mathbf{C}_{11}^{(i)} A_i}{\mathbf{C}_{12}^{(i)}} = \sum_{j=1}^{n} \mathbf{S}_{ij}^{\mathrm{d}} \left(-\frac{\det(\mathbf{C}^{(j)})}{\mathbf{C}_{12}^{(j)}} A_j + \frac{\mathbf{C}_{22}^{(j)}}{\mathbf{C}_{12}^{(j)}} B_j \right). \tag{C.7}$$
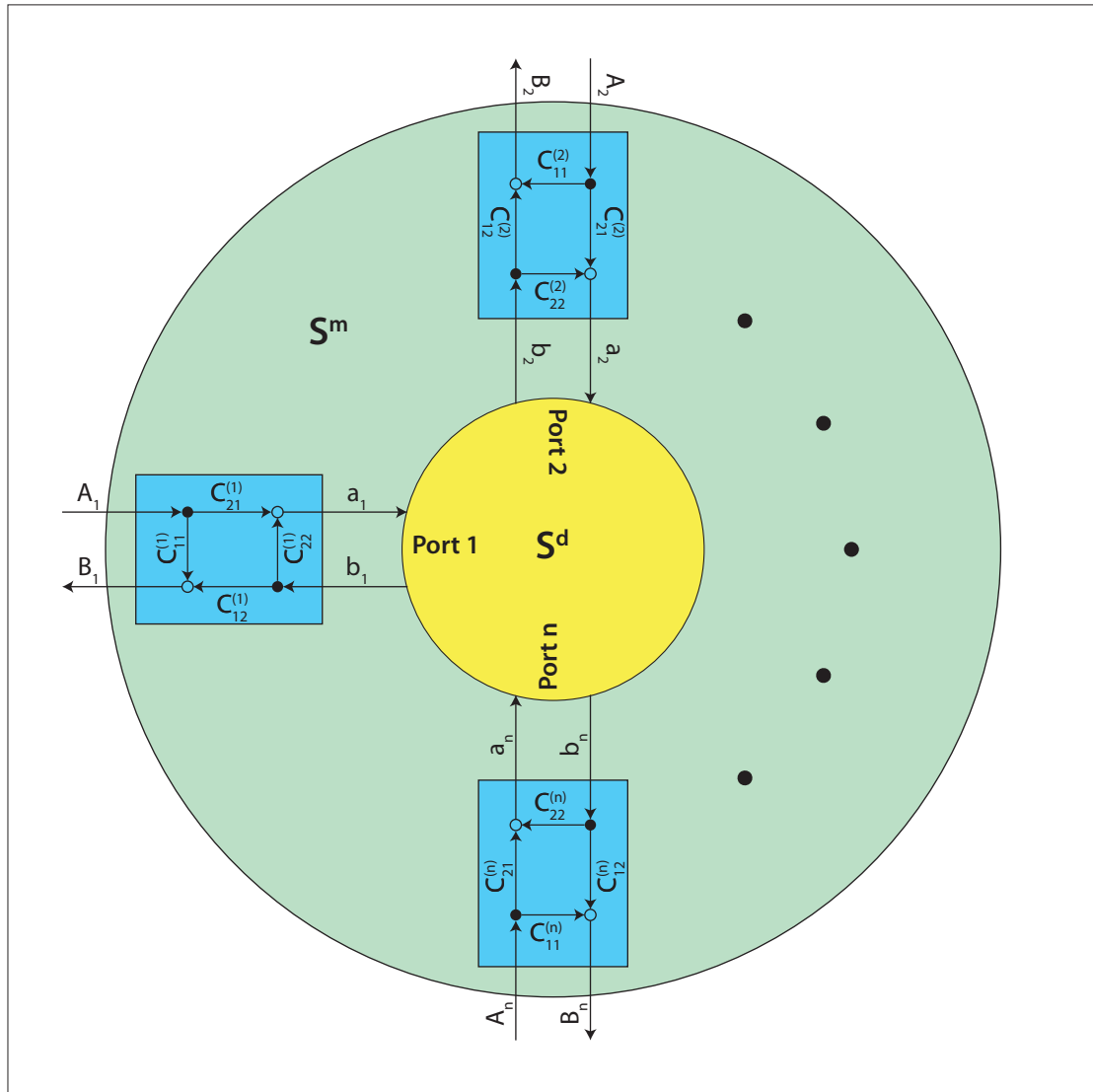
Figure C.1.: Coaxial cables in blue are de-embedded from a general n port network in green to obtain the n port network in yellow

49

Now we look at a situation where only a wave incides at port l. This means

$$A_j = \delta_{jl}A_l. \tag{C.8}$$

Together with the equations (C.1) and (C.7) we get

$$\frac{\mathbf{S}_{il}^{\mathrm{m}} - \delta_{il}\mathbf{C}_{11}^{(i)}}{\mathbf{C}_{12}^{(i)}} = \frac{\mathbf{C}_{22}^{(l)}\mathbf{S}_{ll}^{\mathrm{m}} - \det(\mathbf{C}^{(l)})}{\mathbf{C}_{12}^{(l)}} + \sum_{\substack{j=1 \\ j\neq l}}^{n} \frac{\mathbf{C}_{22}^{(j)}}{\mathbf{C}_{12}^{(j)}}\mathbf{S}_{jl}^{\mathrm{m}}\mathbf{S}_{ij}^{\mathrm{d}} \tag{C.9}$$

where i and l are integers from one to n. This is a system of linear equations for the unknowns $\mathbf{S}_{ij}^{\mathrm{d}}$. The system can be rewritten in matrix form and one obtains equation (5.1).

D. Series resonant circuit

Figure D.1 shows a series resonant circuit. The impedance Z of the resonant circuit is

$$Z = \frac{1}{\mathrm{i}\omega C} + R + \mathrm{i}\omega L. \tag{D.1}$$

Its absolute value is minimal at the resonance frequency ω_s. Since the real part of Z is fixed the absolute value becomes minimal if the imaginary part of Z is zero. This leads to

$$\omega_\mathrm{s} = \frac{1}{\sqrt{LC}}. \tag{D.2}$$

Suppose the resonant circuit is driven at resonance frequency such that the generator supplies the energy dissipated by the circuit. Then the quality factor is defined as

$$Q = \omega_\mathrm{s} \cdot \frac{E_\mathrm{stored}}{P_\mathrm{loss}}, \tag{D.3}$$

where the circuit dissipates the power P_loss in average and stores the energy E_stored. In the following the expressions for P_loss and E_stored are derived. The driving voltage is

$$U(t) = U_0 \mathrm{e}^{\mathrm{i}\omega_\mathrm{s} t}. \tag{D.4}$$

At resonance the impedance of the circuit is R and therefore the current

$$I(t) = \frac{U_0}{R} \mathrm{e}^{\mathrm{i}\omega_\mathrm{s} t} \tag{D.5}$$

flows. The averaged dissipated power is then

$$P_\mathrm{loss} = \frac{1}{2} U(t) I^*(t) = \frac{U_0^2}{2R}. \tag{D.6}$$

The energy E_stored is stored in the electric field of the capacitor and the magnetic field of the inductor. It is given by

$$E_\mathrm{stored} = \frac{1}{2} C \operatorname{Re}(U_C(t))^2 + \frac{1}{2} L \operatorname{Re}(I(t))^2. \tag{D.7}$$

The voltage U_C over the capacitor can be calculated with Kirchhoff's loop rule.

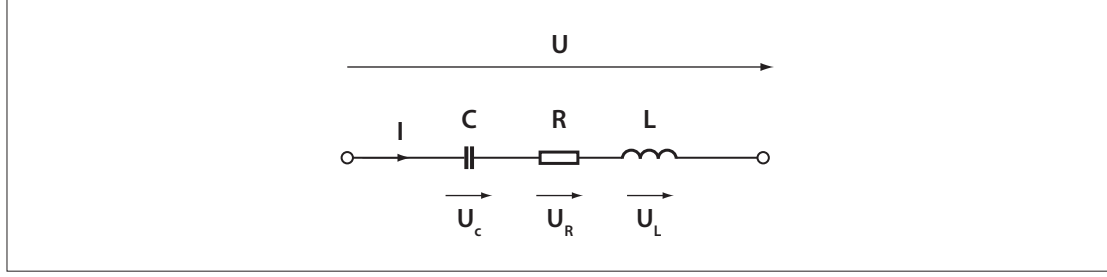$$U_C(t) = U(t) - RI(t) - L\frac{\mathrm{d}I(t)}{\mathrm{d}t} \tag{D.8}$$

Figure D.1.: Series resonant circuit

With the formulas (D.4), (D.5) and (D.8) the expression (D.7) for the stored energy can be written as

$$E_{\text{stored}} = \frac{LU_0^2}{2R^2}. \tag{D.9}$$

The quality factor defined in equation (D.3) is then given by

$$Q = \omega_{\text{s}} \frac{L}{R} = 2\pi\nu_{\text{s}} \frac{L}{R}. \tag{D.10}$$

In the following the admittance of a series resonant circuit is expressed with its quality factor and its resonance frequency. The admittance is

$$Y = \frac{1}{Z} = \left(\frac{1}{\text{i}\omega C} + R + \text{i}\omega L \right)^{-1}. \tag{D.11}$$

The sum can be rewritten on one fraction and we obtain

$$Y = \frac{\text{i}\omega C}{1 + \text{i}\omega RC - \omega^2 LC}. \tag{D.12}$$

By using the equations (D.2) and (D.10) one gets

$$Y = \frac{\text{i}\omega C}{1 + \text{i}\frac{\omega}{\omega_{\text{s}}}\frac{1}{Q} - \left(\frac{\omega}{\omega_{\text{s}}}\right)^2}. \tag{D.13}$$

After some algebraic manipulations the following formula is obtained.

$$Y = \text{i}\omega C \frac{(\omega_{\text{s}}^2 - \omega^2)Q - \text{i}\omega_{\text{s}}\omega}{[(\omega_{\text{s}}^2 - \omega^2)Q]^2 + \omega_{\text{s}}^2\omega^2} \omega_{\text{s}}^2 Q \tag{D.14}$$

With the identities $\omega = 2\pi\nu$ and $\omega_{\text{s}} = 2\pi\nu_{\text{s}}$ this leads to

$$Y = \text{i}2\pi\nu C \frac{(\nu_{\text{s}}^2 - \nu^2)Q - \text{i}\nu_{\text{s}}\nu}{[(\nu_{\text{s}}^2 - \nu^2)Q]^2 + \nu_{\text{s}}^2\nu^2} \nu_{\text{s}}^2 Q. \tag{D.15}$$

E. Transmission line model

A transmission line can be divided into small segments of length Δz. The circuit in figure E.1 models such a segment. The properties are covered by the following quantities.

- The conducting material of the transmission line convert a certain amount of electrical energy into heat. This dissipation is described by the resistance R' per unit length.

- The conductors are separated by an insulator. Since the insulator is not perfect a small current leaks through it. This is described by the admittance G' per unit length.

- If the current through a conductor changes in time a current is induced which reacts against the change. The self-inductance is described by the inductance L' per unit length.

- A voltage across the insulator induces charge. This is described by the capacitance C' per unit length.

In the following we assume that the transmission line is homogenous. Therefore the resistance, the admittance, the inductance and the capacitance per unit length are constant along the transmission line.

The Kirchhoff's loop and point rule applied on a segment of the transmission line give

$$(R' + i\omega L')\Delta z \cdot I(z + \Delta z) + U(z) - U(z + \Delta z) = 0, \tag{E.1}$$

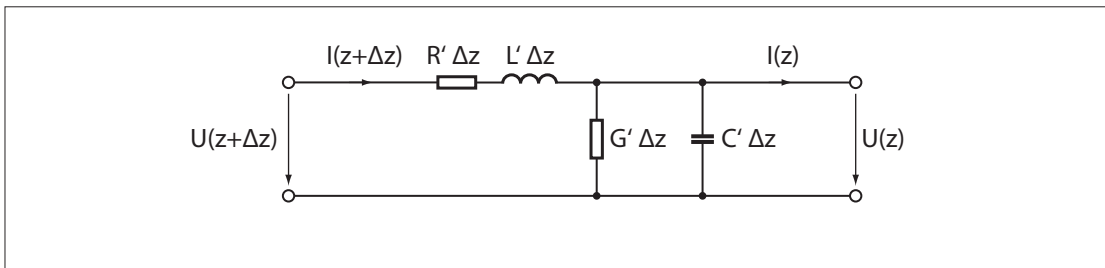$$I(z + \Delta z) - I(z) - (G' + i\omega C')\Delta z \cdot U(z) = 0. \tag{E.2}$$

Figure E.1.: Equivalent circuit for a segment of length Δz of a transmission line

If the segment length Δz goes to zero the equations become

$$\frac{\mathrm{d}U(z)}{\mathrm{d}z} - (R' + \mathrm{i}\omega L') \cdot I(z) = 0, \tag{E.3}$$

$$\frac{\mathrm{d}I(z)}{\mathrm{d}z} - (G' + \mathrm{i}\omega C') \cdot U(z) = 0. \tag{E.4}$$

We have assumed that $U(z)$ and $I(z)$ are continuous and differentiable. The equations (E.3) and (E.4) are two coupled linear differential equations. They can be uncoupled by differentiating (E.3) with respect to z and using equation (E.4). This gives

$$\frac{\mathrm{d}^2 U(z)}{\mathrm{d}z^2} - \gamma^2 = 0, \quad \text{with} \tag{E.5}$$

$$\gamma = \sqrt{(R' + \mathrm{i}\omega L')(G' + \mathrm{i}\omega C')}. \tag{E.6}$$

The solution are two counter propagating damped harmonic oscillations

$$U(z) = C_1 \mathrm{e}^{\gamma z} + C_2 \mathrm{e}^{-\gamma z}, \tag{E.7}$$

since γ is generally a complex quantity. With the formula (E.3) the solution for the current amplitude $I(z)$ is

$$I(z) = \frac{1}{Z_0}(C_1 \mathrm{e}^{\gamma z} - C_2 \mathrm{e}^{-\gamma z}), \quad \text{with} \tag{E.8}$$

$$Z_0 = \sqrt{\frac{R' + \mathrm{i}\omega L'}{G' + \mathrm{i}\omega C'}}. \tag{E.9}$$

The quantity Z_0 is called the characteristic impedance. It is real for lossless transmission lines or for high frequencies. This is often fulfilled in the microwave regime.

The solution (E.7) and (E.8) can be rewritten with the voltage and the current at position zero

$$U(0) = C_1 + C_2, \tag{E.10}$$

$$I(0) = \frac{1}{Z_0}(C_1 - C_2). \tag{E.11}$$

This gives the solution in matrix form

$$\begin{pmatrix} U(z) \\ I(z) \end{pmatrix} = \mathbf{A}_{\mathrm{TL}} \begin{pmatrix} U(0) \\ I(0) \end{pmatrix}, \tag{E.12}$$

with the ABCD-matrix

$$\mathbf{A}_{\mathrm{TL}} = \begin{pmatrix} \cosh(\gamma z) & Z_0 \sinh(\gamma z) \\ \sinh(\gamma z)/Z_0 & \cosh(\gamma z) \end{pmatrix}. \tag{E.13}$$

In the microwave frequency range the relation $R' \ll \omega L'$ and $G' \ll \omega C'$ are often satisfied. Therefore the propagation constant γ can be approximated as

$$\gamma \approx \alpha + \mathrm{i}\frac{\omega}{v_{\mathrm{ph}}} \quad \text{with} \tag{E.14}$$

$$\alpha = \frac{1}{2}\left(\sqrt{\frac{C'}{L'}}R' + \sqrt{\frac{L'}{C'}}G'\right) \tag{E.15}$$

$$v_{\mathrm{ph}} = \frac{1}{\sqrt{L'C'}}. \tag{E.16}$$